DRAFT VERSION FEBRUARY 2, 2008
Preprint typeset using LaTeX style emulateapj v. 10/09/06

PRE-MERGER LOCALIZATION OF GRAVITATIONAL-WAVE STANDARD SIRENS WITH *LISA*: TRIGGERED SEARCH FOR AN ELECTROMAGNETIC COUNTERPART

BENCE KOCSIS
Harvard-Smithsonian Center for Astrophysics, 60 Garden Street, Cambridge, MA 02138

ZOLTÁN HAIMAN
Department of Astronomy, Columbia University, 550 West 120th Street, New York, NY 10027

KRISTEN MENOU
Department of Astronomy, Columbia University, 550 West 120th Street, New York, NY 10027
Draft version February 2, 2008

ABSTRACT

Electromagnetic (EM) counterparts to supermassive black hole binary mergers observed by *LISA* can be localized to within the field of view of astronomical instruments ($\sim 10\,\mathrm{deg}^2$) hours to weeks prior to coalescence. The temporal coincidence of any prompt EM counterpart with a gravitationally-timed merger may offer the best chance of identifying a unique host galaxy. We discuss the challenges posed by searches for such prompt EM counterparts and propose novel observational strategies to address them. In particular, we discuss the size and shape evolution of the LISA localization error ellipses on the sky, and quantify the corresponding requirements for dedicated EM surveys of the area prior to coalescence. The basic requirements of a wide field of view and fast detectors are similar to those for searches being planned for distant cosmological supernovae. A triggered EM counterpart search campaign will require monitoring a several–square degree area. It could aim for variability at the 24–27 mag level in optical bands, for example, which corresponds to 1-10% of the Eddington luminosity of the prime *LISA* sources of $\sim (10^6$–$10^7)\,\mathrm{M}_\odot$ BHs at $z = 1-2$, on time–scales of minutes to hours, the orbital time–scale of the binary in the last 2–4 weeks of coalescence. A cross–correlation of the period of any variable EM signal with the quasi–periodic gravitational waveform over 10-1000 cycles may aid the detection. Alternatively, EM searches can detect a transient signal accompanying the coalescence. The triggered searches will be ambitious, but if they successfully identify a unique prompt electromagnetic counterpart, they will enable new fundamental tests of gravitational physics. We highlight the measurement of differences in the arrival times of photons and gravitons from the same cosmological source as a valuable independent test of the massive character of gravity, and of possible violations of Lorentz invariance in the gravity sector.

Subject headings:

1. INTRODUCTION

The detection by the future *Laser Interferometric Space Antenna* (*LISA*) of gravitational waves (GW) emitted during the coalescence of supermassive black holes (SMBHs) in the mass range $\sim (10^4$–$10^7)\,\mathrm{M}_\odot/(1+z)$ will constitute a milestone for fundamental physics and astrophysics. High angular resolution observations of the nuclei of several dozen galaxies over the past several years have revealed that supermassive black holes (SMBHs) are ubiquitous in local galaxies (see, e.g., the review by Kormendy & Richstone 1995). Mergers are expected to play an important role in the formation and evolution of SMBHs on cosmological time–scales. The number of events that will be detectable by *LISA* is uncertain by orders of magnitude, depending on model assumptions (Haehnelt 1994; Menou et al. 2001; Volonteri et al. 2003; Micic et al. 2007; Sesana, Volonteri, & Haardt 2007; Islam, Taylor & Silk 2004). However, for many events in the above mass and redshift range, *LISA* would be able to measure the masses and spin vectors of the SMBHs, their orbital parameters, and their luminosity distance, to a precision unprecedented in any other type of astronomical observation (e.g. Vecchio 2004; Lang & Hughes 2006). In addition to providing crucial new information for hierarchical structure formation scenarios and black hole astrophysics, the observation of these GW sources would offer new tests of general relativity and cosmology (Hughes & Menou 2005; Berti et al. 2005a,b; Arun et al. 2006a,b).

While the GW signatures themselves are a rich source of information, the secure identification of the LISA source in electromagnetic (EM) wavebands would enable a host of new applications. Traditional astronomical tools could be used to study the nature of these sources in detail, clarifying how the SMBHs grow, evolve, and affect their galaxy environments (e.g. Kocsis et al. 2006). The simultaneous study of photons and gravitons from a single source would also likely probe fundamental aspects of gravitational physics (e.g. Deffayet & Menou 2007).

The single most important unresolved issue is whether counterparts to *LISA* sources will, in fact, be found in electromagnetic (EM) wavebands. The final angular localization by *LISA* itself is relatively poor (typically a few $\times$ 0.1 square degrees at merger), and early studies on counterparts pointed out that this large solid angle will contain many thousands of galaxies, suggesting that identifying the galactic host of the coalescing SMBHs will be difficult, or impossible (e.g. Vecchio 2004). However, recent work has reached much

Electronic address: bkocsis@cfa.harvard.edu
Electronic address: zoltan@astro.columbia.edu
Electronic address: kristen@astro.columbia.edu

more optimistic conclusions. Using *LISA*'s localization of the source within a 3-D error volume (rather than 2-d sky position) reduces the number of candidate galaxies by $\sim 2-3$ orders of magnitude (Holz & Hughes 2005; Kocsis et al. 2006). Furthermore, if the coalescing SMBHs themselves produce bright emission (such as bright quasars), or are associated with some other, similarly rare subset of all galaxies (such as ultra–luminous infrared galaxies [ULIRGs], whose large infrared luminosity may arise from the galaxy merger process that also causes the SMBH binary coalescence), then the identification of a unique counterpart may become feasible for a typical *LISA* source (Kocsis et al. 2006).

Another possibility, raised by Kocsis et al. (2007, hereafter Paper I), is to monitor the sky for EM counterparts in real time, even as the SMBH inspiral proceeds. Various strategies to carry out this monitoring effort are the subject of the present follow–up paper. If the exact nature of counterparts or host galaxies were securely known from ab–initio models, then one could hope to identify them post-merger, e.g. based on the peculiar photometric or spectroscopic signatures. However, such ab–initio predictions are difficult. Searching for a variable or transient EM signal produced during the timed GW–emitting phase could be the most efficient way to identify a secure EM counterpart.

The presence of gas is believed to promote the rapid coalescence of a SMBH binary (see, e.g., Escala et al. 2004, 2005, but see Milosavljevic & Merritt 2003 and the review by Gualandris & Merritt 2007 for the possibility of coalescence without gas, through stellar dynamical processes). If one or both SMBHs continue(s) to accrete gas in the GW-emitting stage, for instance, the coalescing binary may shine as a bright quasar (Kocsis et al. 2006; Armitage & Natarajan 2002) with potential variability on a timescale of $\sim$ hours to days, owing to the inspiraling orbital motion of the binary. This differs from post-merger counterpart scenarios. For example, the merger of two nearly equal–mass SMBHs embedded in a thin accretion disk with a central gap may be expected to produce an X-ray afterglow, delayed by a disk viscous time relative to the merger, i.e. possibly $\gtrsim$ years later (Milosavljevic & Phinney 2005). Importantly for prompt counterpart scenarios, the power emitted in GWs during the final hours of the coalescence is very large, exceeding $10^{-4}\,c^5/G \sim 10^{55}\,\mathrm{erg\ s^{-1}}$. As a result, any coupling of even a small fraction of this unprecedentedly large power to the surrounding gas could produce a luminous counterpart, possibly in the form of a variable EM source.

Motivated by these considerations, in Paper I we developed a formalism (which we call the Harmonic Mode Decomposition, or HMD method) to efficiently compute the time–dependent 3–D localization information contained in the *LISA* data stream. We presented an in-depth study of the potential for pre-merger localizations over the large parameter space of potential sources. In particular, we showed that using the GW inspiral signal accumulated up to some look–back time, $t_{\rm f}$, preceding the final coalescence, one already has a good partial knowledge of the sky position and radial distance to the GW source. Indeed, since the sky position is deduced primarily from the detector's motion around the Sun, we found that angular positioning uncertainties are such that often a source can be localized to within a few square degrees several weeks prior to merger. These conclusions have been confirmed in a recent study (Lang & Hughes 2007) that included the additional effects of spin precession and parameter cross–correlations. These effects, which are ignored in our work, impact localization errors only several days or less prior to merger (resulting in significant improvements at late times).

The main proposal put forward here is to search for an EM counterpart by monitoring LISA source candidates in the $\sim$ 2–3 weeks preceding the merger. We emphasize that in this context, the relevant criterion is not the comparison between the number density of potential counterparts and the *LISA* error box ($\sim 0.1\,\mathrm{deg}^2$ in a typical case), but the much less stringent requirement that the *LISA* uncertainty be comparable to the field of view (FOV) of a wide-field survey instrument (say, $\sim 10\,\mathrm{deg}^2$, such as planned for the Large Synoptic Survey Telescope, LSST)[1]. If this requirement is met, it would be possible to use such an instrument to monitor *LISA* counterpart candidates in real time, during the final stages of the BH merger. The goal of the present paper is (i) to discuss, quantitatively, the feasibility of such a prompt EM counterpart search, and (ii) to identify the issues that will likely drive the observational strategies. In particular, we derive source position uncertainties as a function of time using the results of Paper I, and investigate survey strategies to best utilize this localization information.

The remainder of this paper is organized as follows. In § 2, we summarize and expand on the results of Paper I and present time–dependent *LISA* sky position errors. In § 3, we discuss the possibility of identifying the EM counterpart of the *LISA* source by monitoring the merger with a wide field astronomical instrument. In § 4, we discuss the additional science that would be allowed by a real–time EM counterpart identification (as opposed to identifying a counterpart post–merger). In § 5, we summarize the implications of our findings and conclude.

2. TIME–DEPENDENT *LISA* SKY POSITION ERRORS

The first and most fundamental question in searching for prompt EM counterparts is the accuracy to which the *LISA* source can be localized at various look–back times prior to the coalescence. In this section, we present these time–dependent uncertainties. We use the Harmonic Mode Decomposition method described in Paper I. The reader is referred to that paper for details about the method; here, for completeness, we summarize the main assumptions before describing relevant results.

2.1. *Assumptions*

1. In general, an SMBH inspiral is described by a total of 17 parameters. These include 2 redshifted mass parameters,[2] $(\mathcal{M}_z, \eta)$, 6 parameters related to the BH spin vectors, $p_{\rm spin}$, the orbital eccentricity, e, the source luminosity distance, $d_{\rm L}$, 2 angles locating the source on the sky, (θ_N, ϕ_N), 2 angles that describe the relative orientation of the binary orbit, (θ_{NL}, ϕ_{NL}), a reference time and a reference phase at merger, i.e. at the innermost stable circular orbit (ISCO), $t_{\rm ISCO}$, $\phi_{\rm ISCO}$, and, finally, the instantaneous orbital phase, $\phi_{\rm orb}$ (which specifies the time-evolution of the binary). We denote the look-back time before merger by $t_{\rm f}$. Throughout the paper,

[1] Since the redshift of the source can also be inferred from the LISA distance measurement, it helps if at least photometric redshifts can be measured for all candidates; we will discuss this issue in § 3.2.2 below.

[2] For component masses m_1 and m_2, the total mass is $M = m_1 + m_2$, the reduced mass is $\mu = m_1 m_2/M$, the symmetric mass ratio is $\eta = \mu/M$ and the chirp mass is defined as $\mathcal{M} = M\eta^{3/5}$ (Misner, Thorne, & Wheeler 1973), with redshifted masses written as $\mathcal{M}_z = (1+z)\mathcal{M}$.

all time parameters will be quoted in redshifted units (i.e. as measured by an observer on Earth).

2. The signal for a GW inspiral is determined by the above set of parameters and two additional angles describing the orientation of the *LISA* constellation, (Ξ, Φ). Note that these angles precess with time; indeed, this time–dependence carries all of the sky localization information. Since the period is precisely equal to *LISA*'s orbital period of one year, we need to specify only some reference values (e.g. chosen at the time of the merger, $\Xi_{\rm ISCO}$ and $\Phi_{\rm ISCO}$).

3. We use the circular, restricted post-Newtonian (PN) approximation for the GW waveform (Cutler & Flanagan 1994) keeping only the quadrupole GW harmonic for the GW amplitude. Higher order GW harmonics are negligible if the quadrupole harmonic is within the LISA-frequency band for at least a few months, but can improve uncertainties for large mass binaries with $M_z(\eta/0.25)^{3/5} \gtrsim 2\times10^7 {\rm M}_\odot$ and much shorter observation times (Hellings & Moore 2003; Arun et al. 2007a; Trias & Sintes 2007).

4. We neglect the effects of Doppler phase modulation due to *LISA*'s orbital motion which is an excellent approximation for SMBH inspirals (S. A. Hughes, private communication, 2006; Arun et al. 2007b).

5. We neglect SMBH spins and, in particular, neglect the spin–orbit precession for determinations of the angular parameters. This assumption is useful in simplifying our equations and in focusing on the behavior of pure angular modulation. Including the effect of spin helps reduce uncertainties in the final days and hours of the coalescence (Lang & Hughes 2007).

6. We assume circular orbits ($e = 0$). Although eccentricity is efficiently damped by gravitational radiation reaction (Peters 1964), the presence of gaseous circumbinary disks could lead to non-zero eccentricities for at least some *LISA* inspiral events (Armitage & Natarajan 2005; Papaloizou et al. 2001; MacFadyen & Milosavljevic 2006). For highly eccentric orbits, higher order harmonics appear in the GW phase, which could again lead to improved errors.

7. We fix the start of *LISA* observations at a look–back time $t_{\rm i} \equiv \min\{t(f_{\rm min}), 1\,{\rm yr}\}$ prior to merger.[3] This corresponds to the time when the GW inspiral frequency f crosses the low frequency noise wall of the detector at $f_{\rm min} = 0.03\,{\rm mHz}$, but we limit the initial look–back time to a maximum of 1 yr before merger.

8. We assume that the slow annual amplitude modulation due to *LISA*'s orbital motion can be used to determine the luminosity distance and angular parameters, $p_{\rm slow} = \{d_{\rm L}, \theta_N, \phi_N, \theta_{NL}, \phi_{NL}\}$, while the other remaining parameters, $p_{\rm fast} = \{\mathcal{M}_z, \mu_z, t_{\rm ISCO}, \phi_{\rm ISCO}\}$, are determined independently from the high frequency GW phase, with negligible cross-correlation between the two sets of parameters. This has been verified to be a good assumption up to a few days prior to ISCO, with cross–correlations increasing the localization errors only by a few tens of %. Closer to merger, however, cross-correlations can increase final errors at ISCO by a factor of 2-3 (Lang & Hughes 2007).

9. We follow Barack & Cutler (2004) in calculating the spectral noise density, $S_n(f)$, which includes the instrumental noise as well as galactic/extra-galactic backgrounds. For the instrumental noise, we use the effective non-angular averaged online *LISA* Sensitivity Curve Generator[4] (Berti et al. 2005a), while we use the isotropic formulae for the galactic and extra-galactic background (Barack & Cutler 2004). We do not consider errors from possible theoretical uncertainties (Vallisneri & Cutler 2007), which are negligible at look-back times $t_{\rm f}$ well before $t_{\rm ISCO}$, when the binary separations $r \gg r_{\rm ISCO}$.

10. We estimate the expected parameter uncertainties using the Fisher matrix approach, using the Harmonic Mode Decomposition (HMD) method developed in Paper I (essentially a discrete Fourier transform of the GW waveform with fundamental frequency ${\rm yr}^{-1}$ corresponding to the orbital period of the detector). The main advantage of the HMD method is that the time–dependence of errors can be extracted independently of the specific SMBH binary orbital elements, reducing the computation time by many orders of magnitude. This allows us to survey simultaneously the dependencies on source sky position, SMBH masses and redshift. We carry out Monte–Carlo (MC) calculations with 2×10^4 random samples for the angles $\cos\theta_N, \cos\theta_{NL}, \phi_{NL}$, and $\alpha, \Phi_{\rm ISCO}$. Here α is a time-independent combination of $\Phi(t)$ and $\Xi(t)$, defined as $\alpha \equiv \Xi - \Phi + \phi_N - \frac{3\pi}{4}$. The angles are defined relative to LISA's orbital plane (i.e., relative to the ecliptic), with θ_N and θ_{NL} referring to polar and ϕ_N and ϕ_{NL} referring to azimuthal coordinates. Several thousand values of M and z are considered, in the range $10^5 < M/{\rm M}_\odot < 10^8$ and $0.1 \le z \le 7$. In addition, we ran specific MC calculations to study possible systematic effects with respect to the source sky position (on a grid of several hundred values).

2.2. *Evolution of Error Ellipse*

2.2.1. *Size of the Error Ellipse*

With the above assumptions, we obtain the two–dimensional sky position error ellipses. The time–evolving 1σ errors on the size of the ellipse are shown for a few examples in Figure 1.[5] We also note that the Fisher matrix approach, by construction, approximates the sky position errors (and all other parameter uncertainties) by ellipses. This approximation has been shown for the 1σ uncertainties to be in excellent agreement with the posterior probability distributions for the slow parameters determined from Monte Carlo Markov Chain and Bayesian methods (Cornish & Porter 2006; Vallisneri 2007). Figure 1 shows the gradual improvement in localization, for SMBH coalescences with six different fixed mass and redshift combinations, in the form of the major axis ($2a$), minor axis ($2b$) and equivalent diameter ($2r = \sqrt{4ab}$).

[3] The look–back time throughout this paper is defined to run "backwards" from ISCO, i.e. we set $t_{\rm merger} = 0$ (see Paper I).

[4] `www.srl.caltech.edu/~shane/sensitivity/`

[5] Note that throughout this paper, we show 1σ errors. Higher confidence levels will obviously require covering proportionately larger areas.

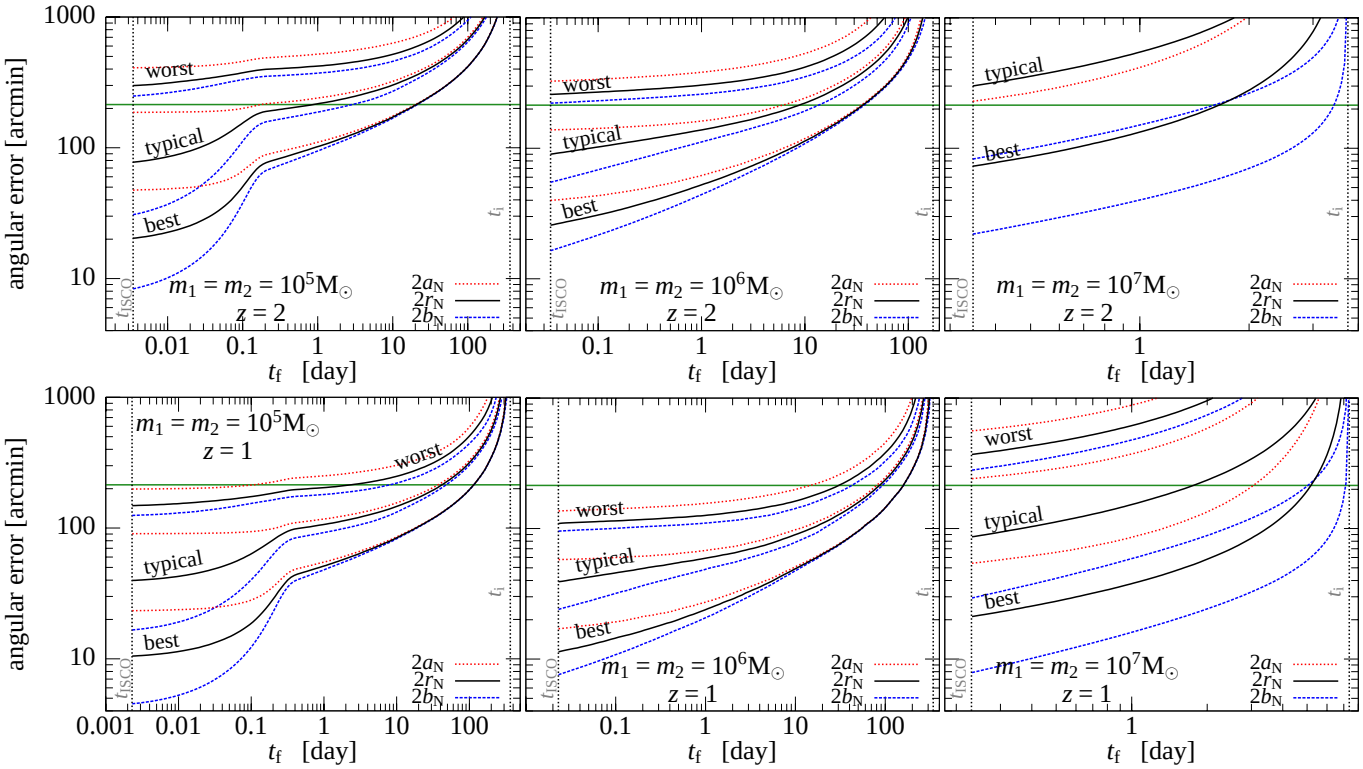

FIG. 1.— Evolution with pre-ISCO look–back time, t_f, of LISA source localization errors for the sky position (major axis $2a$, minor axis $2b$, and equivalent diameter, $2r \equiv 2\sqrt{ab}$, of the error ellipsoid). Six cases with $M = 2 \times 10^{5,6,7} M_\odot$ and $z = 1, 2$ are shown as labeled. Best, typical, and worst cases for random orientation events represent the 10%, 50%, and 90% levels of cumulative error distributions, respectively. The left panels show that the eccentricity of the angular error ellipsoid can change significantly during the last day. The absolute errors are typically small enough to fit in the FOV of a wide–field instrument in the last 1-2 weeks. The horizontal lines show a diameter of 3.57°, which corresponds to localizing the source to within 10 deg^2.

Figure 1 displays results for three separate cumulative probability distribution levels, 90%, 50%, 10%, so that 10% refers to the best 10% of all events, as sampled by the random distribution of the five angular parameters. Note that the levels refer to the parameter in question (i.e. the 10% of all events for which a is best–measured, in general, is different from the 10% of the events for which b is best measured), so eccentricities can not be directly read off from this figure. The evolution of errors scales steeply with look–back time for $t_f \gtrsim 40$ days. For smaller look–back times, errors essentially stop improving in the "worst" (90% level) case, improve with a relatively shallow slope for the "typical" (50% level) case, and improve more steeply in the "best" case (10% level among the realizations of fiducial angular parameters). These behaviors are explained in Paper I; the minor-axis best case approaches the simple $(S/N)^{-1}$ scaling expected in the absence of parameter degeneracies.

In Figures 2 and 3, we show the probability distribution for the errors $2a$ and $2b$ in logarithmic bins at 4 different snapshots: at ISCO, and at 1, 7, and 28 days before merger, using 10^6 random binaries. These distributions are broad, spanning 1–2 orders of magnitude. They are generally asymmetric, skewed right or left for the major and minor axis, respectively. The distribution evolves with look–back time: it is initially peaked, gets flatter and broader approaching merger, and develops a bimodal structure with two peaks. This bimodal nature of the distribution at ISCO is also visible in the histograms of Lang & Hughes (2007), which our Figures 2 and 3 confirm at high resolution. The wide distributions suggest a non–negligible chance of being lucky/unlucky and finding a very well/poorly localized source.

2.2.2. *Eccentricity of the Error Ellipse*

Figures 1, 2 and 3 suggest that the 2D sky localization error ellipsoid is initially circular ($a \approx b$), but the geometry changes significantly during the last stages of the merger. For example, in the typical case (for $z = 1$ and $m_1 = m_2 = 10^6$ M$_\odot$), in the last two weeks, the major axis improves much more slowly than the minor axis. The effect is much more pronounced at lower masses. As the left panels show, the major axis essentially stops improving within the last ∼day, while the minor axis maintains a steep evolution, so that the eccentricity of the 2D angular error ellipsoid changes rapidly (in fact this behavior is even more pronounced if spin precession effects are included, Lang & Hughes 2007). The fact that the error ellipse, in general, changes its eccentricity and its orientation may need to be taken into account in observational strategies (although, of course, as time evolves, subsequent error ellipsoids always lie entirely within the earlier error ellipsoids).

Figure 4 shows the time–evolution of the axis ratio a/b of the 2D angular error ellipsoids for the same mass/redshift combinations as in Figures 1–3. To look for possible correlations between size and eccentricity, we first sorted all binaries according to the total area of the error ellipse into three bins, containing the "small", "medium", and "large" ellipsoids, corresponding to 0–20%, 40–60%, and 80–100% of all events ranked by the instantaneous value of $r = \sqrt{ab}$. Figure 4 then shows the evolution of the 10, 50, and 90 percentiles in eccentricity in each of these three bins separately. The shaded region highlights the distribution of medium–sized ellipsoids, and the thick curves correspond to the median (50%) eccentricities in each bin. Depending on the binary parameters, we find a systematic trend between the size and eccentricity of

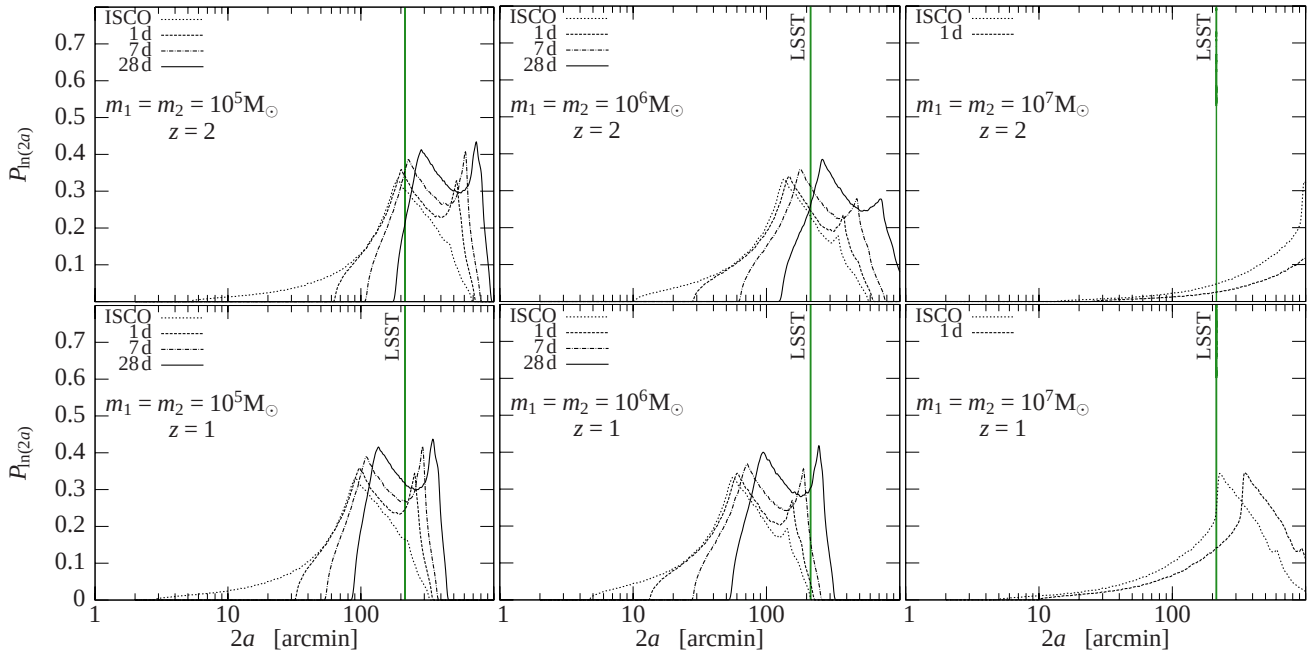

FIG. 2.— Probability density of the 1σ LISA source localization ellipsoid major axis at 4 snapshots: ISCO, and 1, 7, and 28 days before merger. Each curve shows the distribution in logarithmic bins, $\ln(2a)$, calculated using 10^6 random binaries. The vertical line shows the FOV of LSST for comparison.

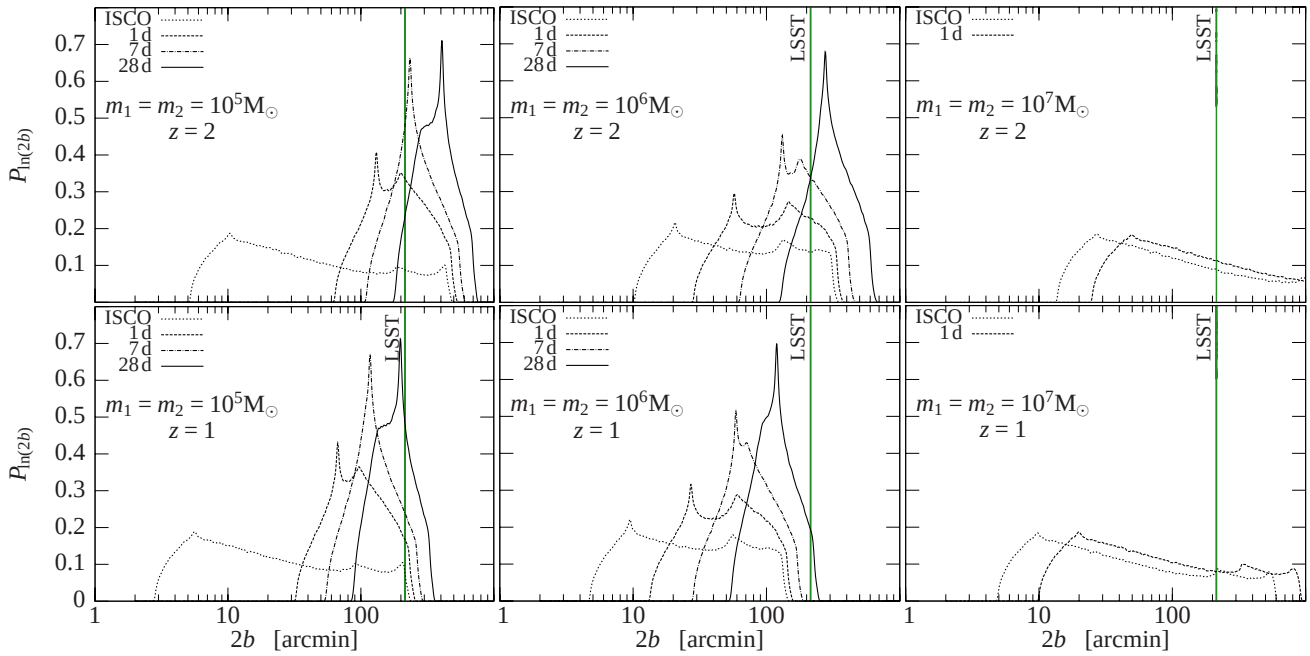

FIG. 3.— Same as Figure 2 but for the sky localization ellipsoid minor axis.

the angular error ellipsoid. Figure 4 shows that if the ellipsoid is relatively small 3 months before merger, then it is very circular, while the larger ellipsoids are more eccentric, but subsequently, at a few days before ISCO, the smaller ellipsoids become just as eccentric as the big ones.

Overall, Figure 4 shows that the eccentricity evolution of the angular error ellipsoid is complicated, but that at the most relevant epochs, i.e. in the last two weeks prior to merger, when the absolute errors have shrunk to interesting levels, the eccentricity increases but remains small until the final day. More specifically, Figure 4 shows that the eccentricity is significant in the beginning, in the first few weeks after the binary enters *LISA*'s frequency band. However, the error ellipse then soon "circularizes", and the eccentricity remains small until the last day before merger. The typical axis ratio decreases below 1.3, 1.1, and 1.01 after two months of observation for the large, medium and small ellipses, respectively. Except for the large ellipses, the eccentricity tends to increase again in the last week before merger. The axis ratio is typically under 1.3 before the last day to merger, with a 10% probability for $a/b = 3$.

2.2.3. *Effects of Mass, Mass Ratio, Upper Harmonics, and Spins*

For high M_z values, the signal frequency at ISCO is low, and the binary coalesces soon after it enters *LISA*'s frequency band. For example, the inspiral of a binary with $m_1 = m_2 =$

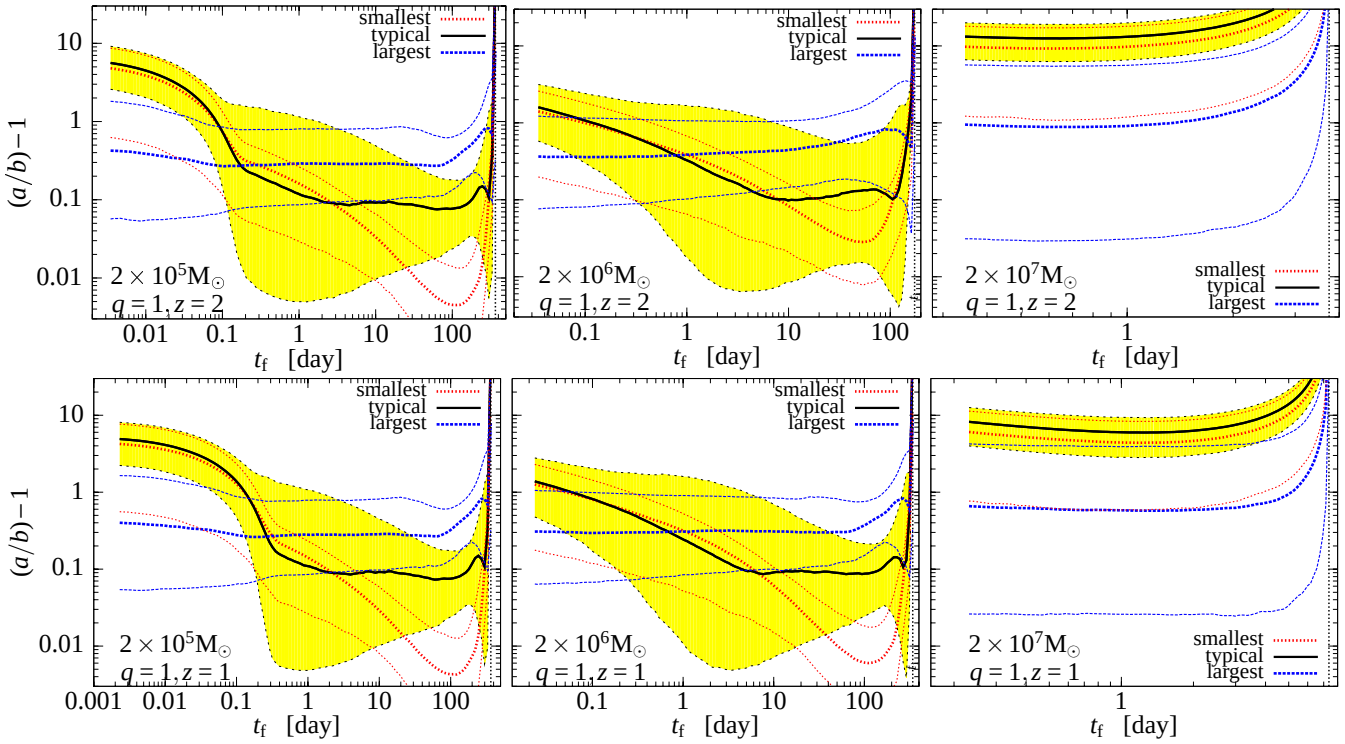

FIG. 4.— Evolution with pre-ISCO look–back time, t_f, of the sky position error ellipsoid axis ratio (a/b) for the same six mass/redshift combinations (and equal masses $q = 1$) as in Figure 1. Each group of three curves corresponds to the 10%, 50%, and 90% levels of eccentricity distributions, based on three bins (smallest, typical and largest) defined by the instantaneous value of the equivalent diameter r at each t_f. Except for small observation times, the eccentricity remains small until the final day. This does not favor a strategy based on "tiling" the field with multiple pointings during a long-term monitoring campaign.

10^7 $M_\odot$ and $z \gtrsim 1$ can only be observed for less than 10 days. In such cases, the sky localization eccentricity does not have time to circularize and the eccentricity remains high (typically $a/b \sim 5$–10) throughout the entire observation. We note however, that higher order GW harmonics beyond the restricted post-Newtonian approximation become relevant in this case, since these harmonics are inside the LISA frequency band much sooner. This improves angular errors greatly for the high mass binaries (Arun et al. 2007b; Trias & Sintes 2007). Due to the increase in observation time, we expect higher GW harmonics to circularize the angular ellipsoid for the more massive binaries.[6]

Although Figures 1–4 correspond to equal mass binaries, we also ran simulations for other mass ratios, $q = m_1/m_2 \sim 0.1$, and found very similar results. A plausible explanation is that two competing effects approximately cancel each other: (1) for fixed total mass M but lower mass ratio η, the instantaneous signal amplitude is lower ($h_{+,\times}(t) \propto \eta$) while (2) the frequency evolves at a slower rate ($\mathrm{d}f/\mathrm{d}t \propto \eta$ and the frequency at ISCO is independent of η) implying that the binary spends more time at larger frequencies where the detector is more sensitive. Relative to the equal mass case, these competing effects approximately cancel out for $q = 0.1$ for both the size and eccentricity of the angular error ellipse. We find differences only for the high mass systems where the total observation time is much larger for $q = 0.1$, leading to a smaller angular error ellipsoid and lower eccentricity.

We expect this description to hold when including spin effects until the final day prior to merger if the observation time is at least months. For high spin binaries, however, spin precession is expected to add an important extra feature to the waveform during the last day which improves the final measurement angular errors by a factor of ~ 3 (Vecchio 2004; Lang & Hughes 2006). In this case, we expect spin precession effects to further increase the angular error eccentricity during the last day. Indeed, recent results by Lang & Hughes (2007) show that the minor axis acquires a long tail toward small values, 10″–1′, indicating that the best events at ISCO will possibly be very elliptic. On the other hand, including spin precession reduces the error eccentricity compared to our estimates if the total observation time is less than a month (R. N. Lang, private communication, 2007). Therefore, spin precession effects will have a tremendous impact on EM follow–up observations, allowing a 1–dimensional tiling of the field with small FOV instruments at late times.

2.2.4. *Sky position dependence*

Figures 1 and 4 show the basic statistics of the expected localization errors when all six angular parameters (2 sky position, 2 angular momentum orientation, and 2 detector orientation parameters) are chosen randomly.[7] This is useful to get an idea of the range of possible accuracies we may have when the LISA data becomes available.

It is also interesting to calculate how the LISA localization errors depend on the actual sky position of the source, since EM counterpart detections can have very different prospects, depending on this position. For instance, it might be difficult to find a counterpart if it lies in the Galactic plane, due to astrophysical foregrounds. On the other hand, a specific example of a preferred direction could be the Lockman

[6] Note that the higher GW harmonics do not change the general expectation that the localization errors can be deduced from the slow amplitude modulation due to the detector motion. Therefore, compared to the restricted PN waveform, it is only the effective increase in the observation time which results in a difference for the localization ellipsoid.

[7] Note that the measured signal depends on only 5 combinations of these angles, therefore only 5 variables are actually varied (§ 2.1).

hole, where the obscuring neutral hydrogen column density is anomalously low.

To examine possible systematic effects with respect to the fiducial sky position, we have divided the (θ_N, ϕ_N) sky into cells and calculated the distribution of errors for each cell by choosing the remaining angular parameters randomly. Surprisingly, in a previous work, Moore & Hellings (2002) showed that no significant trends exist at ISCO as a function of the polar angle θ_N. Our computations (for $m_1 = m_2 = 10^6 M_\odot$ and $10^7 M_\odot$ at $z = 1$) confirm this result to the 10% level, throughout the final 6 months of observation. (Median errors systematically get just slightly worse by less than 10% for sources that lie towards the Ecliptic.) Moreover, we find that localization uncertainties are independent of ϕ_N. This, however, is not surprising since in Paper I we have shown that the LISA measurement depends on the combination $\phi_N - \Phi$, and is otherwise independent of ϕ_N. Therefore the randomness of $\Phi_{\rm ISCO}$ perfectly smears out any systematic effects with respect to ϕ_N. We note that Lang & Hughes (2007) find a very different θ_N dependence: they find Ecliptic equatorial sources to have ~ 2 times larger angular uncertainties than sources near the poles at ISCO. Although Lang & Hughes (2007) employ a different set of assumptions (accounting for correlations and spins, and choosing $\Phi = \Xi = 0$ at the start of the mission), these differences cannot be responsible for the strong θ_N–dependence. The origin of this dependence therefore remains unclear to us.

On the other hand, it is plausible to expect systematic effects in both the Ecliptic latitude and longitude if measuring the longitude relative to the detector position, $\phi_N - \Phi(t)$. We find this to be a useful measure, since once the LISA plans are fixed, $\Phi(t)$ will be known, and $\phi_N - \Phi(t)$ can be converted to Galactic coordinates for each ϕ_N and t. For instance, depending on Φ(January), it might turn out that a "good LISA direction" is in the Galactic plane in January and July, but not during other months.

We calculate error distributions for cells of size $\Delta\cos\theta_N \times \Delta(\phi_N - \Phi_{\rm ISCO}) = 0.1 \times 10^\circ$ and find strong systematic effects: the median localization error improves mostly in the instantaneous LISA plane during the final month, and it is worst in the two orthogonal directions $\pm N_{\rm worst}(t)$, given by $(\theta_N, \phi_N - \Phi(t)) = (120^\circ, 0^\circ)$ and $(60^\circ, 180^\circ)$. This result has also been found independently in a recent study by Trias & Sintes (2007) using non-restricted PN waveforms for high mass binaries. The angular resolution is worst orthogonal to the LISA plane due to geometry: as our viewing angle of the binary changes, due to LISA's orbital and rolling modulation, it causes the smallest change in the waveform since it corresponds to an extremum of the function [measured waveform] vs [viewing angle]. Depending on the source position relative to the plane of the instantaneous orientation of the LISA triangle, the median angular localization uncertainty for $r(t)$, in the case $m_1 = m_2 = 10^6 M_\odot$ and $z = 1$, ranges between 5'–50', 30'–60', 55'–90', 95'–135', and 170'–250' at ISCO, 1 day, 1 week, 1 month, 3 months, and 6 months before ISCO, respectively. Therefore, during the most relevant last week, the area of the sky-position error ellipse can vary significantly, by a factor of 4-100, depending on source position. We find that within the last month, the median errors are roughly rotation–symmetric around $N_{\rm worst}(t)$.[8] Therefore, systematic effects become prominent approaching ISCO because errors improve much more quickly near the LISA plane. Quite remarkably, the errors are small enough very early on everywhere on the sky allowing to decide several months in advance whether the merger will take place in the sensitive region of LISA sky. Therefore, if several coincident inspiral events are identified during the LISA mission, it will be possible to choose which one(s) to monitor with electromagnetic instruments according to which event is projected to have the best LISA precision closer to the merger. (The broader issue of cutting down the number of potential host galaxy counterparts will be discussed in § 3.2.2 below.)

[8] Note that this rotation symmetry might be a consequence of choosing $\Xi_{\rm ISCO}$ randomly in our Monte Carlo simulation (see § 2.1). We also tried fixing $\Phi_{\rm ISCO} - \Xi_{\rm ISCO}$ at some value and found an approximate rotation symmetry in this case as well.

3. TRIGGERED ELECTROMAGNETIC OBSERVATIONS

The results summarized above suggest that it will be possible to identify, prior to merger, a small enough region in the sky where any prompt electromagnetic (EM) counterpart to a LISA inspiral event will be located. Given sufficient "advance notice," it will then be possible to trigger a search for EM counterparts as the merger proceeds (and also during the most energetic coalescence phase).

The several square–degree field will, of course, contain a very large number of sources (a few $\times 10^5$ galaxies in total, at the limiting optical magnitude of ~ 27 mag that may be relevant; e.g. Madau 1999 and discussion below). Having predictions for the spectrum and time–dependence of a coalescing SMBH binary, and therefore knowing what to look for, would obviously greatly help in identifying the counterpart, possibly allowing an identification even post–merger. Such a prediction, however, would require understanding the complex hydrodynamics and radiative properties of circumbinary gas at the relevant small separations of a few to a few thousand Schwarzschild radii. This is a notoriously difficult problem even in the much simpler case of steady accretion onto a single SMBH (e.g. Melia & Falcke 2001). This suggests that the best strategy may be an "open–minded" search for any variable signatures prior and during coalescence.

In the first half of this section, we describe several scenarios in which one may expect an EM signal to be associated with the coalescence of a SMBH binary (see also Dotti et al. 2006). Most of this material in § 3.1 is a review of existing literature. However, we also present some original material, such as calculations of the relevant orbital time–scales (Fig. 5), a rough estimate for the spin magnitude and orientation uncertainties for the binary prior to coalescence (Eq. 1), and we propose that candidates may be selected in advance based on whether or not the binary is expected to experience a large and appropriately directed recoil that would favor bright EM emission (§ 3.1.2).

In most cases, reliable assessments of the nature of the potential EM counterpart are difficult to obtain. What is most important for our purposes is that these scenarios make plausibility arguments for coalescing binaries being able to produce detectable variable signals during their last few weeks prior to merger – either with periodic variations during the inspiral phase, or a strong transient signal during the final plunge/ring–down/recoil phases. In the second half of this section, § 3.2, we give quantitative estimates of the capabilities of planned wide–field instruments to look for such variable signals.

3.1. *Expected or Plausible Variable EM Signatures*

3.1.1. *Periodic Flux Variations During the Inspiral Phase*

The problem of a SMBH binary embedded in an accretion disk has received relatively little attention in the literature. It shares similarities with that of a planet embedded in the protoplanetary disk of its central star, which has been more extensively studied. The case of two near-equal mass SMBH, embedded in a thin, co–rotating disk, has been studied by a few authors. Numerical simulations (Artymowicz & Lubow 1994; Günther, Schäfer & Kley 2004; Escala et al. 2004, 2005) indicate that, in this case, a central hole is expected to open in the disk due to tidal effects and the gas surface density within the binary's orbit could be significantly reduced. In the limit of efficient gap clearing, no EM signal would be expected until after a viscous time ($t \gtrsim$ years) past merger, when the inner edge of the gas disk falls in and starts accreting onto the black hole remnant, producing an X-ray afterglow (Milosavljevic & Phinney 2005).

However, in a more realistic situation, with no perfect azimuthal symmetry, and especially for unequal masses or thick disks, some gas may still flow across the binary's orbit, and ultimately accrete onto one or both SMBHs. It is not unreasonable to expect that this inflowing gas could produce a bright and variable source, with variability correlated with the orbital period. Indeed, the Newtonian potential around the binary will fluctuate periodically, with order unity variations within a radius equal to the binary separation. The gas responds to this periodic perturbation, and a corresponding quasi–periodic flux variability has been proposed on the basis of recent numerical simulations (MacFadyen & Milosavljevic 2006; Hayasaki, Mineshige & Sudou 2007).

Earlier numerical simulations, motivated largely to explain the 12–yr variability of the blazar OJ 287, also found significant mass in–flux across the edge of the central hole (Artymowicz & Lubow 1996; Günther, Schäfer & Kley 2004), especially when the disk gets thick (although these models relate to ~ 1000 times larger separations than the GW-emitting stage of interest here). Likewise, in the planetary context, close pre-main-sequence binary stars are expected to clear central holes in their proto-planetary disks, but Jensen et al. (2007) argue that material can flow from the circumbinary disk across the gap to explain the observed 19–day variability of the young binary UZ Tau E.

There are other scenarios that may plausibly produce a variable signature related to the binary orbit. For example, Armitage & Natarajan (2002) examine the case of a highly unequal mass binary, and argue that a significant amount of gas may be driven in by the merger if it is initially present interior to the orbit. Another way to promote variable signatures associated with the influence of the binary's orbital motion is to allow gas to flow in even as gravitational radiation rapidly shrinks the binary's orbit. This may be possible if the circumbinary disk is geometrically thick (or advection-dominated), with a viscous timescale much shorter than traditional thin accretion disks.

Assuming that variability is indeed present, what is the expected period of this variability? Again, the answer is uncertain, but a reasonable guess is that the variability will be related to half the orbital time–scale of the binary, corresponding to the periodic quadrupolar perturbation of the gravitational potential.

In Figure 5 we show the time (Δt) spent by a binary with a total mass of $10^{5,6,7}$ $M_\odot$, redshift $z = 1$, at each orbital period t_{GW} (in logarithmic bins of t_{GW}). The plots show cases

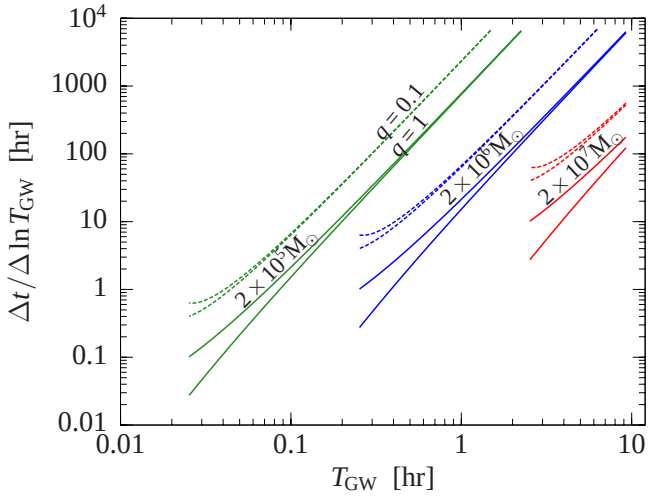

FIG. 5.— The time spent (in hr) per logarithmic GW cycle-time bin during the inspiral for $M = 2 \times (10^5, 10^6, 10^7) M_\odot$ (as labeled), $q = 1$ (solid) and 0.1 (dashed) for $z = 1$ in the restricted 2.5PN approximation. In each case two curves with the same style correspond to the two extremes: maximum aligned and anti-aligned spins; a general case lies in between these extremes. T_{GW} is the GW cycle time in hours. The curves end at $t_i = 1$ yr or at $f_{min} = 3 \times 10^{-5}$ Hz, corresponding to $T_{GW} = 9.3$ hr. Note that the number of GW cycles can be estimated as $N_{cycles} = y/x$, from the x and y–axis values corresponding to each curve.

with mass ratios of $q = 1$ (solid) and 0.1 (dashed). The various curves of the same type show the upper and lower bound of the time-evolution depending on the magnitude and orientation of BH spins. The presence of spin modifies appreciably only the final day of the merger.

Quite remarkably, Figure 5 shows that the expected EM variability timescale is in a very fortunate range for detection: between several minutes up to 10 hours within the last year of merger. Detecting slower variations would require several exposures over exceedingly long time–periods, while detecting faster variations (of the same amplitude) would require much higher sensitivity per unit exposure time. If a periodic electromagnetic variation is found within this range, e.g. for an AGN in X-rays, it would indicate evidence for an SMBH binary approaching coalescence. The evidence would be especially convincing if this nearly periodic variable "light–curve" tracked the known, nearly periodic GW emission, with a significant cross–correlation between the periods of the two waveforms. The EM lightcurve may perhaps even follow the slow decrease in period, related to the GW chirp, shown in Figure 5.

On the basis of the relatively well–defined nature of these potential counterparts, it may even be interesting to carry out, well before the LISA mission becomes operational, systematic searches for such quasi-periodic behavior with the various all sky variability surveys currently being planned.

3.1.2. *Transient Signatures During Final Coalescence*

Perhaps the most promising phase for the emergence of bright EM counterparts to SMBH merger events is, in fact, during or shortly after the violent final coalescence stage. This is the most energetic phase of the binary's evolution, with typically $\sim 10^{58}$ ergs of gravitational radiation released to the environment in a short $\sim 10^3$ s. There are at least two ways to couple this energetic outburst to the immediate gaseous environment of the SMBH binary (see also Milosavljevic & Phinney 2005).

A few percent of the binary system's rest mass is lost when the binding energy of the two holes is carried away by GWs.

Most of this loss occurs during the final cycles of inspiral, the plunge and subsequent ring-down. Gas bound to the SMBH's binary would thus experience a sudden reduction in the mass of the central object, on a timescale typically much shorter than the longer (local) dynamical timescale on which this gas can respond. Although this sudden disturbance is of moderate amplitude ($\sim$ a few %), it is a potential source of transient variability associated with the coalescence, depending on details of the disturbed surrounding gas properties (Bode & Phinney 2007).

A second, and possibly more direct and promising avenue to couple the energetic GW burst at coalescence to the SMBH binary's environment is through the GW recoil/kick experienced by the system. The accumulation of linear momentum leading to the final recoil builds during the final cycles of inspiral, the plunge and subsequent ring-down, so that it appears as quasi-instantaneous except for any gas that may be located in the immediate vicinity of the coalescing binary. The magnitude of the kick is determined by the mass ratio, the magnitude of the spins, and the relative orientation of the spin and orbital angular momentum vectors. The recoil kicks can be calculated accurately using numerical relativity (e.g, Baker et al. 2006). The final BH velocity is found to reach 170 km/s for no spins (González et al. 2007), and 2500–4000 km/s for high spins in special configurations (Campanelli et al. 2007; Brügmann et al. 2007). For comparable mass binaries with large spins and arbitrary orientation, a recoil > 500 km/s has a 30% probability (Schnittman & Buonanno 2007). If the spin axis is aligned with the angular momentum, as maybe the case in gas rich mergers, then the recoil is expected to be $\lesssim 200$ km/s (Bogdanović et al. 2007, and see § 3.2.2 below). Even for a modest recoil velocity of 100 km/s, this amounts to $\sim 10^{53}$ ergs of mechanical energy that can in principle be deposited in the environment as a SMBH remnant of $\sim 10^6$ M$_\odot$ ploughs through. The EM signatures that may emerge from such interactions are difficult to evaluate *a priori* since they will depend on many details, such as the properties of the gas that remains bound to the recoiling SMBH, the geometry of the recoil system with respect to its environment, and possibly the remnant BH spin. We will simply note here that these EM counterparts are not necessarily bound by the Eddington limit traditionally applied to steady systems, if the recoil energy is deposited fast and efficiently enough for the event to adopt an outflowing/explosive character.

For the present discussion, it is interesting to ask whether the final recoil magnitude and direction can be estimated in advance, and to determine whether it lies in the plane of the binary, where a gaseous disk may be preferentially located. If so, then this advance knowledge could possibly be used to pick the events that are most likely to produce a transient EM counterpart. Since recoil velocities are determined by the mass ratio, spin magnitudes and orientations, the question is whether these parameters can be estimated with sufficient precision in advance. Without specific computations, we can estimate the advance uncertainties for these parameters using simple scaling arguments. The mass ratio is determined from the 1PN effect, hence it is a "fast parameter" that will likely improve quickly with time, close to $(S/N)^{-1}$ (see § 2.1). Spin effects arise at 1.5PN order, implying that the binary spins are also "fast parameters". The final errors on the spin magnitudes are excellent (see Lang & Hughes 2006), better than 1%–6%–20% for z = 1–3–5 if $m_1 = m_2 = 10^6$M$_\odot$. Even the final spin angle uncertainties have not been estimated previously, but we can assume that they are not much worse for large spins than the angular momentum orientation uncertainties ($\delta\theta_L, \delta\phi_L$), since the two are coupled through precession, and precession was shown to help in reducing the ($\delta\theta_L, \delta\phi_L$) errors. If the spin magnitude is chosen randomly, then the spin orientation measurement error is 3.5 deg for $m_1 = m_2 = 10^6$M$_\odot$ at $z = 1$ (R. N. Lang, private communication, 2007). We assume conservatively that the evolution of spin errors scale with $(S/N)^{-1}$ until the last day before ISCO. According to Paper I, $S/N \propto t_{\rm f}^{1/3}$. In this case

$$\delta{\rm spin}(t_f) \simeq \left(\frac{t_f}{t_{\rm ISCO}}\right)^{1/3} \delta{\rm spin}(t_{\rm ISCO}), \qquad (1)$$

with $t_{\rm ISCO} = 33\,{\rm min} \times (M_z/(4\times 10^6 {\rm M}_\odot))$. For $m_1 = m_2 = 10^6$M$_\odot$ at $z = 1$, we find $\delta{\rm spin} \simeq 1\% \times [t_f/(33\,{\rm min})]^{1/3}$. i.e. spin magnitudes will be determined to $\sim 8\%$ at 10 day before ISCO. For the direction, ~ 10 deg (~ 20 deg) precision can be achieved 10 days before ISCO, if the final uncertainty at ISCO is 1.3 deg (2.6 deg). This information could thus in principle be used to focus on events with specific magnitudes and/or directions for the expected recoil, in an effort to maximize the likelihood of finding bright EM counterparts.

3.2. *Searching for Variable Signals with Wide Field Instruments*

3.2.1. *Basic Parameters for a Variability Search*

The most obvious observational strategy to catch a prompt EM counterpart, especially in the absence of robust theoretical predictions, is to blindly and continuously monitor the source area, through coalescence, for variable sources. The requirements for such a monitoring – large FOV, and a fast camera – coincide with those of searches for distant Supernovae (SNe) in the optical bands. Motivated by the latter, there are several instruments being built or planned with specifications that could prove suitable for a *LISA* counterpart search. Table 1 shows a non-exhaustive list of facilities, either planned or being built, that have a several square–degree field of view and may be suitable for a *LISA* counterpart search.

According to the arguments in the previous section, a coalescing binary may produce some variable signature in the last two weeks before ISCO. The amplitude and period of any variability, however is highly uncertain. In view of this uncertainty, it is interesting to work backwards, and compute the expected brightness of a variable signal that is some fixed fraction of the Eddington luminosity. An Eddington-luminous SMBH at $z = 1-3$, with a mass of $(10^6$–$10^7)\,{\rm M}_\odot$, assuming a 10% bolometric correction, would appear as a $\sim$ 22–25 mag point source in the optical bands. This implies, for example, that if the variable signal is $\sim 10\%$ of the Eddington luminosity, then we need sensitivities corresponding to 24–27 mag. Ten times lower mass BHs would require sensitivities of 26–29 mag. This variability is to be detected on an orbital time–scale, which is between several minutes to several hours (Fig. 5).

Scaling from the sensitivities shown in Table 1, assuming $S/N \propto \sqrt{t}$, we see that a sensitivity of $\sim 25-27$ mag can be reached in $\sim$ 1min to $\sim$ 1hr integrations with Pan–STARRS and with LSST. We conclude that an LSST–class instrument, repeatedly integrating over the *LISA* area, would be able to detect a variability that corresponds to $\sim 10\%$ of the Eddington luminosity and follows the period of the binary's orbit.

Figures 1 and 4 show that the eccentricity of the *LISA* error box may be significant during the last day or for high–mass

TABLE 1
WIDE FIELD ELECTROMAGNETIC INSTRUMENTS

Name	FOV (deg^2)	bands	mag. limit (exp)	start date	reference
High Energy Transient Explorer-2	0.9, 1.6 srad	soft, hard X-ray, γ	$8\times10^{-9}\,\frac{\mathrm{erg}}{\mathrm{cm^2 s}}$	2000	space.mit.edu/HETE
Galaxy Evolution Explorer	1.2	Near, Far UV	21-22 (1 hr)	2003	www.galex.caltech.edu
Palomar–Quest	3.6×4.6	U,B,R,I,r,i,z	17.5-21.0 (140sec)	2003	Baltay et al. (2007)
XBoötes Survey	9.3	X-ray	$(1\text{–}8)\times10^{-15}\,\frac{\mathrm{erg}}{\mathrm{cm^2 s}}$	2005	www.noao.edu/noao/noaodeep /XBootesPublic
SkyMapper	2.3×2.4	u,v,g,r,i,z	20.6-21.9 (110sec)	2007	www.mso.anu.edu.au/skymapper
South Pole Submillimeter Telescope	1	sub-mm (350–850)μm	1 mJy (18-27 hr)	2007	cfa-www.harvard.edu/$\sim$aas/tenmeter
Low Frequency Array	20	radio (10–240)MHz	(0.03–2)mJy (1 hr)	2007	www.lofar.org
Pan-STARRS-1	2.5×2.5	g,r,i,z	24 (1 min, 5σ)	2008	pan-starrs.ifa.hawaii.edu
Gamma-ray Large Area Space Tel.	2 srad	γ	$6\times10^{-9}\,\frac{1}{\mathrm{cm^2 s}}$ (1yr)	2008	glast.gsfc.nasa.gov
Dark Energy Survey	2.2×2.2	g,r,i,z	24 (100 min,5σ)	2009	www.darkenergysurvey.org
Kepler	105	430–890nm	24 (150 min,5σ)	2009	kepler.nasa.gov
Large Synoptic Survey Telescope	10	u,g,r,i,z,Y	27 (1 hr, 5σ)	2014	www.lsst.org
Joint Dark Energy Mission	15	6 optical + 3 NIR	27 (1 hr)	2016	universe.nasa.gov/program /probes/jdem.html
Wide Field Imager	1	350–1800 nm	24 (110 min)	2017	sci.esa.int/science-e/www/object /index.cfm?fobjectid=39692
Energetic X-ray Imaging Survey Tel.	154 x 65	X-ray	$2\times10^{-14}\,\frac{\mathrm{erg}}{\mathrm{cm^2 s}}$	2020	exist.gsfc.nasa.gov
Square Kilometer Array	1	radio (20–200)GHz	1 μJy (1 hr)	2020	www.skatelescope.org

NOTE. — The table shows EM instruments, existing, being built, or planned, that have a several square–degree field of view and may be suitable for a *LISA* counterpart search. The 3rd column shows the observational wavelength bands, and the 4th column shows the sensitivity that can be reached in these bands in the indicated integration time at the quoted S/N (derived from information at the websites listed for each instrument in the 6th column, when possible).

SMBHs with $M \gtrsim 2\times10^7\mathrm{M}_\odot$, with the more uncertain (major) axis longer by up to a factor of several than the better determined (minor) axis. This may impact the plausible duration of any triggered monitoring. If the telescope is rapid enough, then one requires only that the minor axis fits within the FOV (assuming that the FOV is spherical), since it will be possible to tile the rest of the *LISA* ellipse by a few extra pointed observations, displaced along the major axis. On the other hand, if the required integration time is comparable to the expected orbital period, then performing such a tiling would mean shallow observations that may miss the variability. In this case, the monitoring campaign can start only after the major axis has shrunk below the linear size of the FOV.

Figures 6 and 7 display advance warning time contours for typical (50%) and best case (10%) events, adopting the LSST FOV as a reference. Advance warning time contours are logarithmically spaced, with solid contours every decade and the shaded region highlights the (M,z) region where at least 10–day advance notice will be available. The top panel of Figure 6 shows that 10 day advance warning to cover the full error ellipsoid with a single LSST pointing is possible for a large range of masses and source redshifts, up to $M\sim3\times10^7\mathrm{M}_\odot$ and $z\sim1.7$. The bottom panel shows that the (M,z) region in which this same 10 day warning is limited to the minor axis of the error ellipsoid reaches to somewhat higher redshifts. Figure 7 shows how far the advance warning concept can be stretched, by focusing on the 10% best cases of random orientation events. The top panel shows that a 10 day warning to cover the full error ellipsoid with a single LSST-type pointing is possible up to $z\sim3$ for masses around $M\sim10^6\mathrm{M}_\odot$. The bottom panel shows that the (M,z) region in which the same 10 day warning is restricted to just the minor axis of the error ellipsoid reaches out to comparable redshifts, for a similar range of masses.

As explained above, a unique variable EM signal could be produced in the last stages of the merger. Figures 6 and Figure 7 show that requiring a warning of just one day would extend considerably the range of masses and redshifts for which a single LSST-type pointing is sufficient, out to $z\gtrsim5$ for the best events. However, as we mentioned above, Lang & Hughes (2007) find that in the last day, parameter correlations can degrade the errors by a factor of 2–3, but this degradation is more than offset by the factor of several improvement in the errors caused by spin precession (for high spin). Therefore, our localization errors for the last day are overly optimistic, by a factor of 2-3, for low spin mergers, but are conservative for high–spin mergers. Also, the issue of eccentricity turns out to be most important in this regime (i.e. for localizing the best events ~1 day prior to ISCO, especially for high spins, see § 2.2.3). In this case, requiring the FOV to cover only the minor axis would allow going out to $z\sim8$.

It should be possible to significantly improve on the above magnitude requirements, if the signal is indeed close to periodic at t_{GW}. This is because the above calculation requires the flux variations to be detectable for any individual source in the LSST FOV. A lower–amplitude variable signal would be lost in the noise for any individual source (i.e. it will be consistent with photometric noise). Fitting to a sinusoid–like template would require much less sensitivity. Even in the absence of a precise template for the EM emission, one could use the GW waveform itself (or variations of it). Cross–correlating the EM flux with the peaks and troughs of the GW waveform should allow one to recover such below–the–threshold variability, effectively decreasing the smallest detectable variability amplitude by a factor of $\sim\sqrt{N_{\mathrm{cycles}}}$, where $N_{\mathrm{cycles}}\approx10^{3,2,1}$ is the number of orbital cycles for the binary during the last two weeks, for $M=10^{5,6,7}\mathrm{M}_\odot$, respectively (see Fig. 5).[9] This type of template matching could presumably be attempted in various regions of the EM spectrum (see Table 1 for a few possibilities).

3.2.2. *Cutting Down on the Counterpart Candidates*

The above scenario so far envisions monitoring all sources in a few square degrees, in $\sim$ hourly intervals, for $\sim$ two weeks prior to and around ISCO. This wide field will contain a

[9] Note that $\sqrt{N_{\mathrm{cycles}}}$ scaling is correct only for constant modulation power per cycle, which might not be the case for the EM variations.

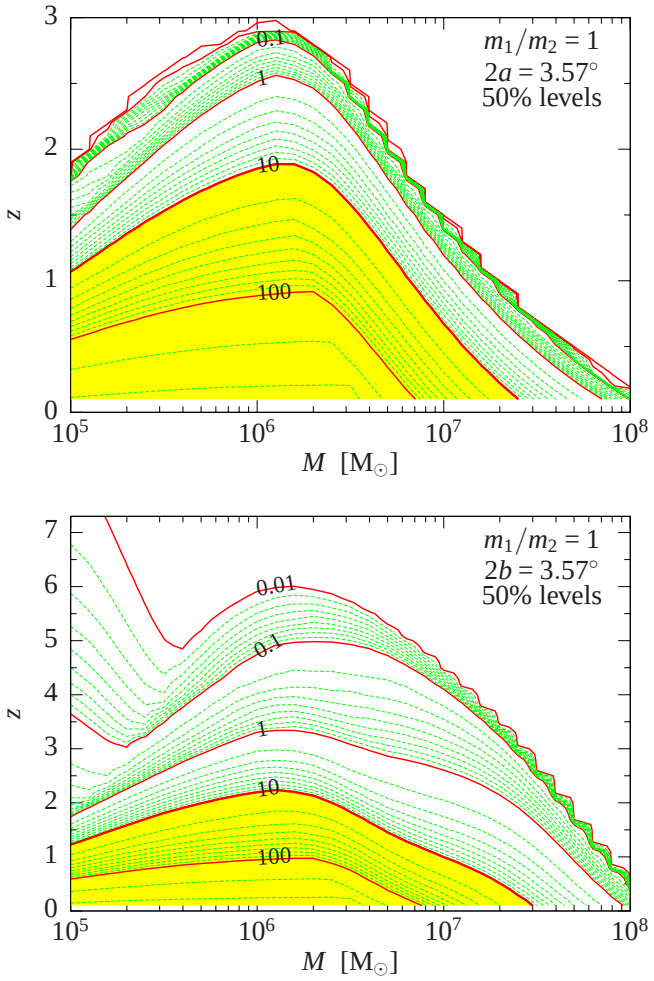

FIG. 6.— Contours of advance warning times in the total mass (M) and redshift (z) plane, for typical events (50% level of cumulative distributions for random orientation events) with SMBH mass ratio $m_1/m_2 = 1$. The contours trace the look–back times at which the major axis ($2a$, top panel) and the minor axis ($2b$, bottom panel) of the localization error ellipsoid first reach an LSST-equivalent field-of-view (3.57°). The contours are logarithmically spaced in days and 10 days is highlighted with a thick curve.

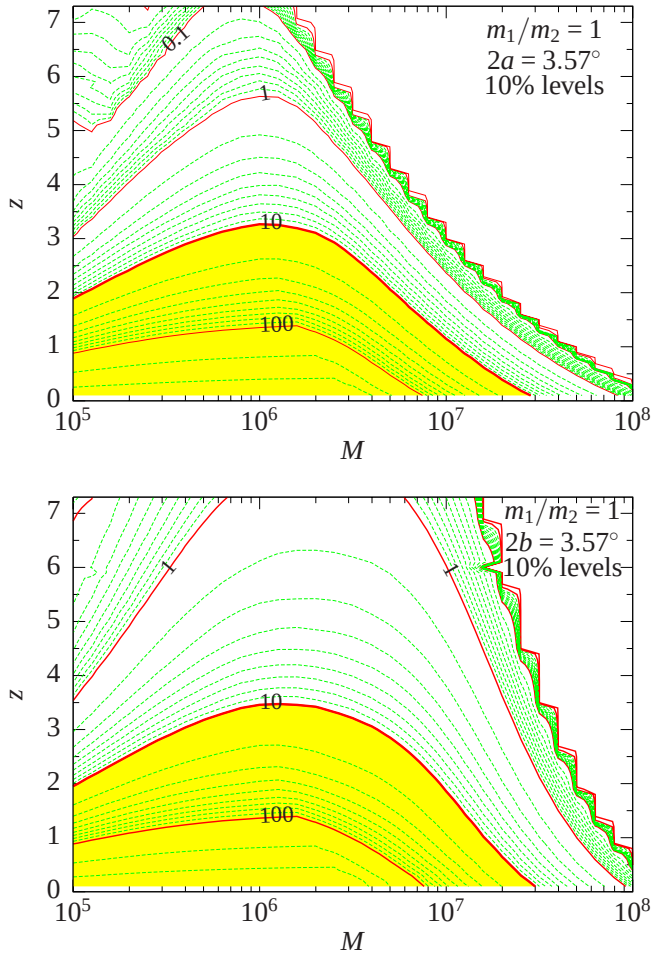

FIG. 7.— Same as Figure 6, except that results for the best (10% cumulative level) events are shown.

very large number of galaxies. As seen earlier, the interesting optical magnitude limit may be $\sim 25-27$, for variability at the level of $1-10\%$ of the Eddington limit. The surface density of galaxies at this magnitude is known from deep optical observations to be about $\sim 10^6\,\mathrm{galaxies}/(10\,\mathrm{deg}^2)$ (e.g. Madau 1999). While this large number of possible candidates may seem daunting, there are several ways to significantly shrink the candidate list. We enumerate these options in this section.

Final Angular Localization Cut. In Figures 6 and 7 we showed the advance warning times when the source localization can be first covered with a $10\,\mathrm{deg}^2$ instrument. However not all galaxies are going to be relevant in this region eventually, since the area of the error ellipsoid shrinks continuously (Fig. 1). For $m_1 = m_2 = 10^6\mathrm{M}_\odot$ at $z = 1$, for instance, the $10\,\mathrm{deg}^2$ localization is typically reached at $t_\mathrm{f} \approx 86$ days. The (10–90)% distribution levels of the sky position uncertainty later decrease to $\delta\Omega = (0.1\text{–}1)$ and $(0.6\text{–}7)\,\mathrm{deg}^2$ at $t_\mathrm{f} = 1$ and 10 days before ISCO (Fig. 1). During the last day, the size of the ellipsoid decreases by another factor of ~ 3 for a source with large spins (Lang & Hughes 2007). Therefore the number of candidates among the galaxies within the original $10\,\mathrm{deg}^2$ field decreases to a fraction (6–70)%, (1–10)%, and (0.3–10)%, at 10 days, and 1 day before merger, and at ISCO, respectively. Obviously, these cuts can only be applied progressively as the merger progresses, always abandoning candidates that move out of the shrinking error ellipse, and not immediately at the beginning of the monitoring campaign.

Photometric Redshift Slices. All of the survey instruments listed in Table 1 should be able to observe the field in several bands, and, for example, LSST should be able deliver photometric redshifts of all sources with an accuracy of $\delta z \lesssim 0.05$ (see, e.g. Huterer et al. 2006). If LSST has already surveyed the target area before the *LISA* event, then galaxies will have tabulated magnitudes and photo–z's already. These data may, however, not pre–exist, or may not go deep enough (if the SMBH system has too small a mass). But the cumulative exposures of this particular $\sim$ deg^2 field during a monitoring campaign should be sufficient to reach target errors already in approximately the first day of monitoring.

Importantly, *LISA* will deliver the luminosity distance $d_L(z)$ with high accuracy. In Figure 8, we show the errors on distance as a function of time. For a flat ΛCDM cosmology with $(\Omega_\Lambda, \Omega_m, h) = (0.7, 0.3, 0.65)$ the redshift uncertainty is given by $\delta z = (0.81, 1.6)\delta d_\mathrm{L}/d_\mathrm{L}$ for $z = (1, 2)$, respectively, provided that $\delta z > 0.005$ (Kocsis et al. 2006). Few percent errors are thus reached several days prior to ISCO, except for the worst–case events, in the entire mass range, $10^5 - 10^7$ M$_\odot$, out to $z = 2$. However, the distance determination is ultimately limited by weak lensing uncertainties due to fluctuations in the dark matter density along the line of sight, shown as a horizontal line in Fig 8 at $\delta z_\mathrm{wl} = (0.025, 0.097)$ for $z = (1, 2)$,

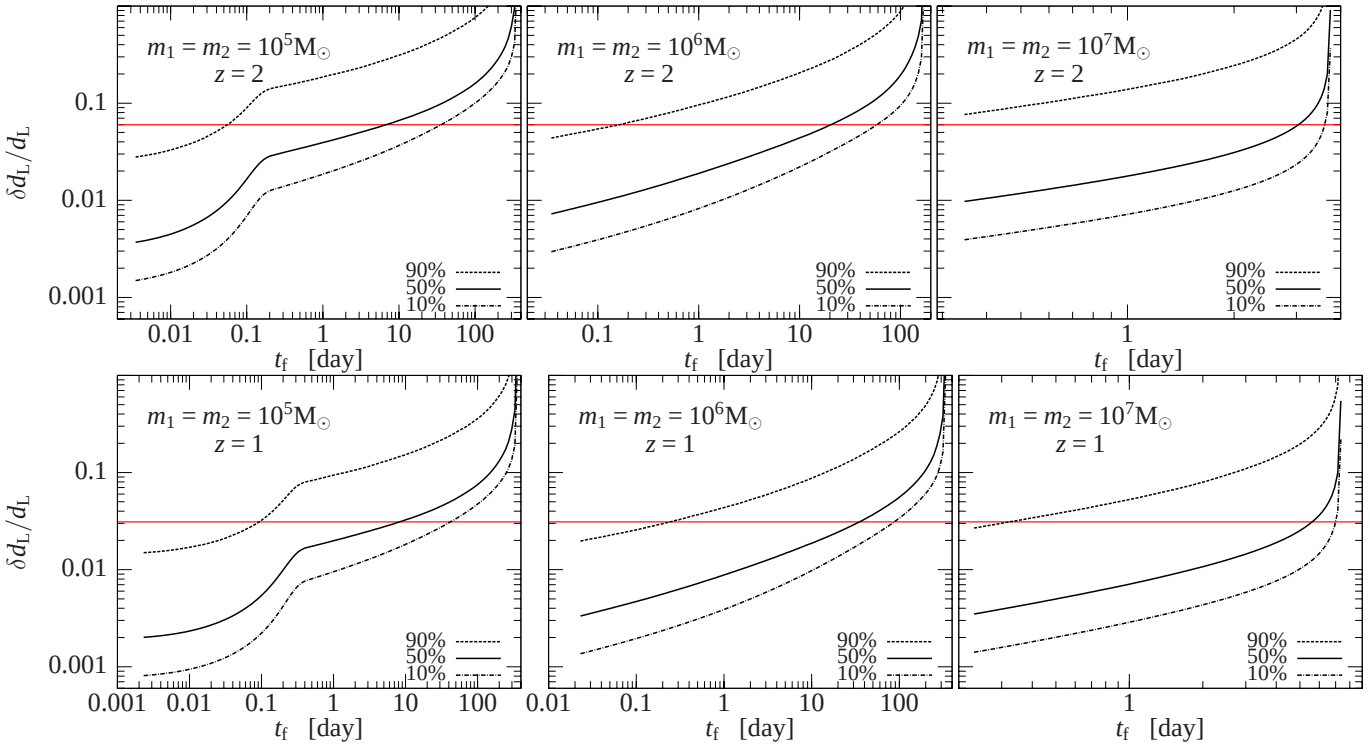

FIG. 8.— Evolution with pre-ISCO look–back time, t_f, of LISA errors on the luminosity distance $d_L(z)$ for $m_1 = m_2 = (10^5, 10^6, 10^7)$ $M_\odot$ and $z = (1, 2)$ as labeled. The 10%, 50%, and 90% levels of cumulative error distributions for random orientation events are shown. Horizontal lines delineate the level of uncorrected weak lensing uncertainties.

respectively. The weak lensing uncertainty cannot easily be corrected by more than a factor of $\sim 40\%$ (see Dalal et al. 2003; Kocsis et al. 2006; Gunnarsson et al. 2006). Once the *LISA* uncertainty decreases below this limit, the total redshift error will not improve. The redshift distribution of optical galaxies at 27–28 mag is already known from deep observations (e.g Coe et al. 2006, using the Hubble Ultra Deep Field), with roughly 1–10% of them falling in a radial shell of width $\delta z \sim 0.05$ around redshift $z = 1$–2, hence photometric redshifts will offer a factor of $\sim$ 10–100 reduction in the number of candidates.

Expected Luminosity Range. Since *LISA* will also measure accurate BH masses prior to the merger (the masses are "fast parameters", see § 3.1.2) it may be possible to roughly estimate the magnitude of the host galaxy from the known empirical correlations between galaxy properties and SMBH mass. For example, extrapolating from the sample of nuclear SMBHs in the local universe, a $\sim 10^6$ $M_\odot$ SMBH is expected to reside in a galaxy with a spheroid mass $\sim 10^9$ $M_\odot$, or absolute magnitude $M_B \sim -16$ (Ferrarese & Merritt 2000), corresponding to an apparent optical magnitude of $m \sim 28$ at $z = 1$.

A large fraction of the galaxies will not have luminosities consistent with the mass–luminosity relationship and the BH masses determined by LISA, allowing to efficiently reduce the number of counterparts. Using Eq. (19) of Ferrarese & Ford (2005), we find that the *B*-band spheroidal luminosities are $M_B = (-12.7^{+1.5}_{-2.2}, -15.1^{+1.6}_{-1.1}, -17.5^{+1.0}_{-0.65})$ for SMBH masses $M_{\rm SMBH} = 2 \times 10^{5,6,7} M_\odot$. Note, that the errors are (by far) dominated by the uncertainties in the $M_{\rm SMBH}$–M_B relationship, and not the LISA measurement errors, with $\delta M_{\rm SMBH}/M_{\rm SMBH} \lesssim 10^{-4}$. In order to obtain the total luminosity, we must divide the spheroidal luminosity with the spheroidal/total luminosity ratio S/T. This ratio depends on the galaxy morphology, orientation, and luminosity. For the low–luminosity spheroids that will host the SMBHs with $M_{\rm SMBH} = 10^{5-7} M_\odot$, a conservative assumption is $S/T = 0.1$–1 (Benson et al. 2007). Integrating the observed luminosity function of galaxies between these M_B bounds (Ryan et al. 2007, using their fits for faint galaxies at $z = 1$, $\Phi^* = 26.1 \times 10^{-4}\,{\rm Mpc}^{-3}$, $M_B^* = -22.4$, $\alpha(z) = -1.12 - 0.12z$, and $P = -1.00$, $Q = 1.72$ given by Lin et al. (1999) for $q_0 = 0.1$, and extrapolating this relationship to low luminosities) and using the cosmological comoving volume element (Eisenstein 1997)

$$N_{\rm counterpart}(z) = \delta\Omega\delta z \frac{\partial^2 V_{\rm co}(z)}{\partial z \partial\Omega} \int_{M_{B,\rm min}-2.5\log(S/T)_{\rm max}}^{M_{B,\rm max}-2.5\log(S/T)_{\rm min}} \phi(M_B, z) {\rm d}M_B \quad (2)$$

gives $N_{\rm counterpart}/{\rm deg}^2 = 10^3 \times (7.8, 3.7, 1.7)$ and $10^3 \times (10, 3.6, 1.2)$ for $M_{\rm SMBH} = 2 \times 10^{(5,6,7)} M_\odot$, $\delta z = 0.05$ and for $z = 1$ and 2, respectively. If a bulge/disk decomposition is also available to constrain S/T (Benson et al. 2007), then $N_{\rm counterpart}$ is reduced by another factor of ~ 2. Therefore imposing bounds on the range of both the luminosity and the redshift of the counterpart reduces the number of counterparts significantly. Incorporating the angular localization cut above leads to a total of $N_{\rm counterpart} \sim 10^3$–$10^4$ at 10 days before merger, 100–1000 at 1 day, and 1–1000 at ISCO.

We caution, however, that before applying cuts on candidates, one should be well aware that the relation between total SMBH mass and spheroidal luminosity is currently known only for nearby galaxies, selected by observational feasibility criteria. Clearly, the relation can be different for rare objects of a transitional nature, such as SMBHs in the last few weeks of their merger.

Expected velocity dispersion. There is observational evidence for a tight correlation between the SMBH mass, M, and the large scale bulge velocity dispersion of galaxies, σ (Gebhardt et al. 2000). By contrasting M, as measured by

LISA, with σ obtained from galactic spectra, a major fraction of the galaxy candidates could be ruled out. Using equation 20 in Ferrarese & Ford (2005), and extrapolating to lower masses, we find $\sigma = (50 \pm 5, 81 \pm 4, 130 \pm 1)$, for $M = 2 \times 10^{5,6,7} M_\odot$, respectively. In comparison, the velocity dispersion for observed galaxies ranges between $\sigma \sim (60$–$400)\,\mathrm{km/s}$ (Sheth et al. 2003). Since we expect there will be many more galaxies with low velocity dispersion, a very efficient reduction of $N_{\rm counterpart}$ will be only possible for the most massive detected SMBHs. Unfortunately, the measurement of velocity dispersions for faint galaxies is extremely difficult in practice. It may be feasible only for the larger mass BHs, and presumably after longer–integration spectra are obtained well after the merger. As before, we caution that the relation between total SMBH mass and the velocity dispersion is unknown for rare objects of a transitional nature, such as SMBHs in the process of coalescence.

Quasar counterparts. If the *LISA* source is producing a continuous near–Eddington luminosity with fluctuations at the few percent level, then most likely, it will appear as a point source (i.e. a faint quasar) and the host galaxy will not be detectable. The bright point source in the nucleus, with ~ 24 mag, will outshine the galaxy. Kocsis et al. (2006) found that the typical *LISA* error box ($\delta\Omega = 0.3\,\mathrm{deg}^2$, $\delta z = 2.5\%$), for a merger event produced by $\sim 10^6$ $M_\odot$ SMBHs at $z = 1$ would statistically contain ~ 1 quasar with at least 10% Eddington luminosity; the ~ 30 times larger area ~ 2 weeks before merger will contain ~ 30 such quasars. These quasars could be identified in advance, and monitored separately for variability with smaller–field of view instruments.

Orbital Eccentricity as Indication of Circumbinary Gas. In 2D simulations of circumbinary disks, Armitage & Natarajan (2002) and MacFadyen & Milosavljevic (2006) find that the interaction of the binary with the ambient gas produces eccentricity (in the orbit of both the gas and the binary). The eccentricity leaves a strong imprint on the GW waveform (Barack & Cutler 2004; Vasúth & Majár 2007). Moreover, it is a "fast parameter" since it modifies the spectrum of the signal on the binary orbital timescale (see § 2.1). Therefore we expect that the *LISA* data–stream should be able to discover such eccentricity several months before merger and thus alert us to the occurrence of a gas–driven inspiral.

Spin and Orbital Plane Alignments as Indication of Ambient Gas. Prior to the merger, the two SMBHs may reside in two bulges, which are driven together during the galaxy merger by large–scale torques (e.g., Dubinski et al. 1996). As a result, the orbital plane of the binary SMBH may be aligned with the plane of the galactic remnant. Indeed, in gas rich mergers, the binary plane may align with the plane of the disk (Bogdanović et al. 2007). Moreover, these authors argue that the interaction with the gas also aligns the individual BH spins in the direction of the orbital angular momentum. Therefore the relative orientation of the binary orbit, spin vectors, and embedding galaxy may be valuable observables. In particular, if the measured spin vectors are found to align with the orbital angular momentum, it may indicate that a sufficient amount of gas was present in the history of the merger. Moreover, in the case of alignment, the direction of the recoil kick at merger is in the orbital plane, making the kick–triggered variability discussed in § 3.1.2 more plausible. Conversely, misaligned spins may indicate that the merger is dry, and an EM signal might not as easily accompany the GW event. Note that a $\pm 20\,\mathrm{deg}$ triple alignment between the spins and orbital momentum by chance has a mere 9×10^{-4} probability. In case there are several coincident inspirals present in the LISA data-stream, a favorable EM follow-up candidate could thus be chosen according to a criterion for potential EM activity based on the observed relative alignments.

In Figure 9, we show the accuracy with which we will know the inclination of the SMBH orbital angular momentum, in advance of the merger, as specified by the two angles (θ_L, ϕ_L). When considering the individual EM candidates in the LISA error volume, one-by-one, the EM information allows to set the sky position errors $(\delta\theta_N, \delta\phi_N)$ to essentially negligible values. Therefore, it is meaningful to calculate the 2D error ellipsoid for (θ_L, ϕ_L) by neglecting correlations with $\delta\theta_N$ and $\delta\phi_N$. Figure 9 then shows that we will know the inclination remarkably well in advance. One may therefore envision focusing on galaxy candidates that exhibit inclinations similar to that of the SMBH binary. This will be feasible only if the host galaxy is actually detected and resolved (i.e. if the SMBH binary does not produce near–Eddington emission whose PSF completely hides the galaxy). The angular size of small elliptical galaxies at $z = 1-3$ with optical magnitudes ~ 27 is expected to be 0.1–0.5 arcseconds (see, e.g., simulations by Kawata & Gibson 2003), which cannot be resolved from the ground. However, by $z \sim 1$, most of the host spheroids may be surrounded by much larger disks. For example, the 20 kpc diameter disk of a galaxy like our own Milky Way would extend beyond 2 arcseconds at $z = 1-3$, and could thus be resolved. Again, one can envision separately monitoring with smaller field–of–view instruments a few of those galaxies (if any) whose disks appear to be closely aligned with the orbital plane of the SMBH binary.

In conclusion, the alignment of spins (indicative of the presence of gas) and the alignment of orbital momentum with the plane of the galaxy can be very helpful in choosing the most likely host galaxy candidates. Note, that a $\pm 20\,\mathrm{deg}$ coincidence between the GW and EM measured orbital orientation has a 3% probability, thereby allowing a very effective cut to be made on the candidates.

Galaxy Overdensity as Indication of Enhanced Merger Rate. Another possibility is to focus on galaxy clusters within the few square degrees of interest. There may be a few to a few tens of known galaxy clusters in this area. Combining with the photometric redshift information, $\Delta z = 0.05$, there are on average $N_{\rm cluster}/\,\mathrm{deg}^2 = 0.2$ and 0.01 clusters within this shell, at $z = 1$ and 2, respectively (e.g. Holder, Haiman, & Mohr 2001). The probability that a randomly chosen galaxy has undergone a recent merger is significantly larger in a cluster than in the field; again, it would make sense to separately monitor the dense cluster environments with smaller FOV telescopes.

4. MOTIVATIONS AND NEW FUNDAMENTAL TESTS OF GRAVITY

We have argued that real-time triggered searches for EM counterparts to SMBH binary merger events observed by LISA will be technically feasible, at least for a subset of all such events. Observational strategies to achieve such identifications constitute major astronomical endeavors, however. It is thus important to clarify the nature of the additional science that could be enabled by real-time identifications. We describe two important motivations for pre-merger localizations here.

The first motivation is simply coincidence. Post-merger identification of host galaxies will likely rely on active nucleus variability or on a statistical association with rare galac-

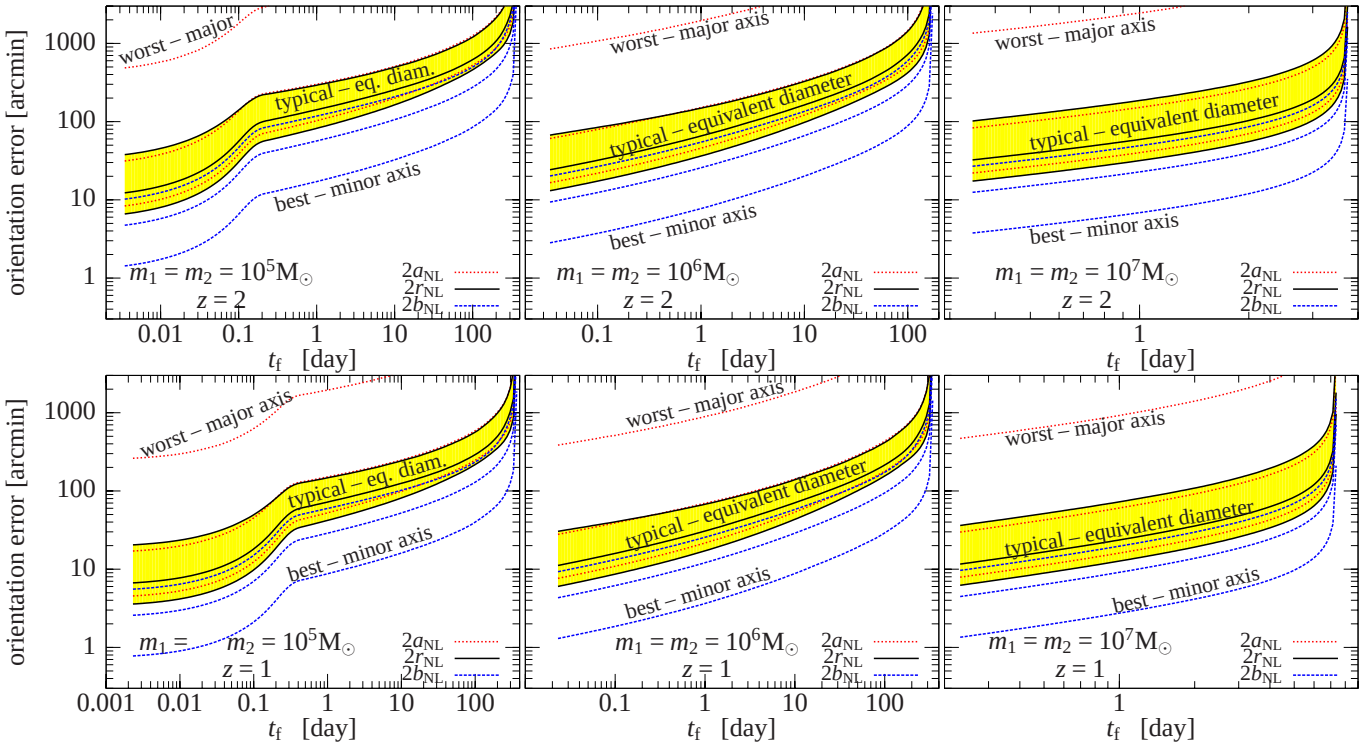

FIG. 9.— Evolution with pre-ISCO look–back time, $t_{\rm f}$, of LISA errors for the orientation of the orbital plane of the SMBH binary relative to the line-of-sight. The inclination and rotation uncertainties are correlated leading to an error ellipsoid with major axis, $2a_{\rm NL}$, equivalent diameter $2r_{\rm NL}$ and minor axis $2b_{NL}$. Best, typical, and worst cases for random orientation events represent the 10%, 50%, and 90% levels of cumulative error distributions, respectively. The range spanned by the $2r_{\rm NL}$ distribution is highlighted for clarity. The figure shows that the binary inclination angle can be precisely localized very early on, to within degrees, allowing a selection of prime host galaxy candidates that have a similar inclination.

tic objects (e.g. quasars, ULIRGs, X-ray or starburst galaxies; Kocsis et al. 2006; Dotti et al. 2006). Depending on the nature of the AGN variability or the specific galactic attribute one is willing to associate with a SMBH binary merger, possibilities for chance coincidences may remain uncomfortably high. The combination of space (sky location) and time coincidence for a prompt EM counterpart that is gravitationally-timed with a SMBH merger should considerably reduce the risks of chance coincidences and would thus likely be the most secure way of identifying a truly unique counterpart and host galaxy. This is particularly important in this context, with observations of a rare transient astrophysical phenomenon that has never been observed before, whether gravitationally or electromagnetically. Secure counterpart identifications are also crucial if one is to perform new fundamental tests of gravitational physics with these events, such as comparisons between electromagnetic and gravitational Hubble diagrams (Deffayet & Menou 2007).

The second important motivation is that the detection of prompt electromagnetic counterparts itself may provide additional opportunities for testing gravitational physics on cosmological scales. We highlight here one such new test, based on the measurement of photon and graviton arrival times from the same cosmological source. As we already emphasized (see §3.1.2) the most violent and energetic phase of the SMBH binary merger will be the final coalescence of the two BHs. Let us assume for simplicity that a luminous burst of light is generated at the same time as the most luminous burst of GWs is emitted by the coalescing binary system. If gravitons propagate at a speed lower than that of light, a delay in the arrival time of the burst of gravitons, relative to the burst of photons, may become apparent after propagation over cosmological distances.

One specific scenario in which this is expected is if the graviton possesses a non-zero rest-mass (e.g, Pauli & Fierz 1939).[10] Assuming that Lorentz invariance is satisfied by the massive gravity theory under consideration, we can infer the bound that can be set on the graviton mass, for a given value of the delay between photon and graviton arrival times. Let us write the light travel time to a cosmological standard siren as η (i.e. the conformal time, e.g. Eisenstein 1997) and the velocity of gravitons as $c_g < c$, where c is the speed of light. By definition, we have

$$\frac{c_g}{c} = 1 - \frac{\Delta t}{\eta}, \tag{3}$$

where $\Delta t > 0$ is the delay in graviton arrival times. The corresponding Lorentz factor is

$$\gamma \equiv \frac{1}{\sqrt{1-(c_g/c)^2}} \simeq \sqrt{\frac{\eta}{2\Delta t}}, \tag{4}$$

so that from $\gamma m_0 c^2 = hf$, one could deduce the graviton rest mass m_0 from the GW frequency, f, and any measured delay, Δt. Note that, using the conformal time η can be expressed with redshift for a given cosmology (e.g. Eisenstein 1997), and no other cosmological factors enter this calculation.

Without any special treatment, it appears unlikely the burst of GWs can be isolated and thus accurately timed to better than about a dynamical timescale for the coalescing SMBH binary (i.e., one final GW cycle). This timing uncertainty will thus set a limit on the minimum graviton rest mass that can be constrained from delays in arrival times. Adopting the inverse

[10] Building a satisfactory Lorentz-invariant theory of massive gravity remains a challenge. Possibly more successful Lorentz-violating versions have also been proposed (e.g, Dubovsky et al. 2005).

of the frequency at ISCO as the limiting timing uncertainty, $f_{\rm isco} = 2.2 \times 10^{-(2,3,4)}$ Hz, for an SMBH binary with total mass $M = 10^{5,6,7} M_\odot$ at $z = 1$, respectively, for which $\eta = 11.6$ Gyr, we find that bounds on the graviton mass based on arrival time delays are possible as long as $m_0 \gtrsim (14, 4.5, 1.4) \times 10^{-25}$ eV or in terms of Compton wavelength $\lambda_c \lesssim (28, 89, 280)$ pc, respectively. This bound on the graviton mass is less stringent, than the 1 kpc value derived from the deviations that would emerge in the phasing of massive GW waveforms (Berti et al. 2005a; Will 2004). In addition, any systematic delay in the emission of the burst of photons, which must causally follow the gravitational event and thus the burst of gravitons, could significantly reduce the quality of the constraints on m_0 based on differences in arrival times between photons and gravitons. In fact, in the absence of any quantitative information on such systematic delays at the source, one will be inevitably reduced to model–dependent statements, with specific emission scenarios, unless observations were to reveal an unambiguous propagation effect (with the burst of photons significantly preceding the burst of gravitons).

In principle, however, a possibility exists for more accurate relative timing of the photon and graviton signals. Before coalescence, gas present in the near environment of the SMBH binary would be gravitationally perturbed in such a way that it could radiate a variable signal with a period closely matching that of the leading-order quadrupolar perturbation induced by the coalescing binary. In this case, independently of the details of the electromagnetic emission process, it may be possible to match the periods of the electromagnetic and GW signals. The offset in phase between the Fourier components of the two signals with similar frequencies could thus be used to effectively calibrate the intrinsic delay in electromagnetic emission at the source. Any drift in arrival-time with frequency between the gravitational and electromagnetic chirping signals, as the source spans about a decade in GW frequency during the last 2 weeks before merger (see Fig. 5), could then be attributed to a fundamental difference in the way photons and gravitons propagate on cosmological distances. Another immediate advantage of this frequency matching is that there is no need to isolate a luminous burst of GWs and to associate it with a corresponding burst of photons in the observed signals. Instead, the various phases of late inspiral and coalescence can be tracked via the GW signal, so that the relative timing of the gravitational and electromagnetic signals may be known to within a fraction of the binary's dynamical time. Of course, it is difficult to assess the accuracy of this matching and tracking with frequency without a more detailed analysis. However, what is clear from our previous discussion is that if the delay in electromagnetic emission at the source can be efficiently calibrated and the absolute timing of both signals can be reduced to less than the binary's orbital period, then the direct comparison of signals could provide constraints on the graviton mass, m_0, of comparable or even better quality than those obtained from the phasing of the GWs alone (Berti et al. 2005a; Will 2004).

It is important to emphasize that the above limits on the value of the graviton mass, m_0, are strongly theory-dependent. In our discussion, as in the analyses of Berti et al. (2005a) and Will (2004), it was assumed that the finite value of the graviton mass has negligible effects on the rate of decay of the binary or other observable properties of the GW signal (such as polarization). Furthermore, Lorentz invariance was explicitly used to relate the delay in arrival times of gravitons to their rest mass, m_0. These various assumptions can be violated in various theories of modified gravity, whether massive or not. We will mention a few possibilities of interest here in that they could be phenomenologically tested.

In braneworld models with extra dimensions available to gravity beyond a large, cosmological "cross-over" scale (e.g., Dvali et al. 2000), from the Kaluza-Klein mechanism, massless higher-dimensional gravitons may start behaving like 4D-massive particles once they travel distances comparable to the theory cross-over scale. There would not be any single rest mass associated with 4D-massive gravitons, so that the specific constraints discussed above or in Berti et al. (2005a) would not strictly apply. That is, after cosmological propagation, the relation between arrival time and GW frequency may be more complex than assumed in equation (4). Even though Lorentz invariance has been extensively tested for standard model fields, the possibility remains that Lorentz symmetry is violated in the gravity sector, especially on cosmological scales. Such apparent gravity sector Lorentz violations emerge in braneworld scenarios, if the phenomenology is incorrectly interpreted from a 4D-spacetime point of view (e.g. Chung, Kolb & Riotto 2002; Csáki et al. 2001). Independently of higher-dimensional scenarios, specific Lorentz-violating theories of gravity in 4D have also been proposed in recent years, e.g. with a vector-tensor character (e.g. Bekenstein 2004; Jacobson & Mattingly 2004).

In this context, it is thus significant that electromagnetic counterparts to SMBH binary mergers, together with the opportunity to match and track the gravitational and electromagnetic signals in frequency, may offer unique tests of Lorentz violations in the gravity sector. It may be possible, as the SMBH binary decays toward final coalescence, spanning a range of frequencies, to measure the delays in graviton vs photon arrival times as a function of increasing GW frequency, f. Therefore, the consistency of Eq. (3) with the special relativistic relation $\gamma m_0 c^2 = hf$ could be tested explicitly, potentially revealing empirical violations of Lorentz invariance for gravitons propagated over cosmological scales. Clearly, to have any chance to perform such new tests of gravitational physics, one will need to identify the electromagnetic counterparts as early as possible. This may be one of the strongest motivations behind ambitious efforts to localize these rare, transient events well before final coalescence.

5. DISCUSSION AND IMPLICATIONS

In this paper, we have considered the possibility of localizing coalescing SMBH binaries in real time, by using the gravitational waves detected by *LISA* to trigger searches for electromagnetic counterparts using wide–field instruments. The idea presented here is that such searches may reveal a time-variable source – showing either quasi–periodic brightness variations during the inspiral stage, or a transient "burst" during the coalescence itself – and that this may allow identification of a unique counterpart.

We first analyzed the behavior of the time–evolving localization error prior to the merger. As the binary evolves in time, the signal-to-noise ratio, S/N, per unit time of the GW detection increases rapidly. Therefore the measurement precision of physical parameters, such as the 3D position, inclination, and spins can improve quickly as the merger approaches. We have calculated the size and shape of the 3D localization ellipsoid, and its distribution for arbitrary binary orientations and sky positions, as well as how these uncertainty distributions evolve before the merger. We found that for typical sources at

z = 1–2, $\sim$ 10 days before merger, the distance measurement precision reaches its limiting value $\delta z_{wl} \sim$ (2–10)% imposed by weak gravitational lensing. Redshift errors subsequently decouple from the sky position errors, and the 3D localization ellipsoid aligns with the line of sight. The sky position error decreases below 10 deg^2, 10 days before merger, for a large range of masses, $10^5 \leq M/\mathrm{M}_\odot \leq 5\times10^6$, at redshifts $z \leq 1.5$. We have also found that the sky position error ellipse is nearly circular after the first few weeks of observation, except for the final $\sim$day before the merger, especially for the small ellipsoids with favorable sky positions and inclinations. During the final day, the minor axis of the sky ellipse shrinks more quickly, especially for large BH spins (Lang & Hughes 2007), creating an eccentric sky position error ellipse. Finally, we found that the source position can be important: localization improves quickly for sources that lie in the plane defined by the *LISA* triangle, but remains much poorer in the perpendicular direction.

We then analyzed the prospects for electromagnetic monitoring of this sky area to look for prompt counterparts and host galaxy candidates. It will be possible to estimate the time of the merger to better than an hour precision already several months in advance of merger. The expected number of galaxies that would be present in the GW localization region is up to 10^6 during the last weeks. However, we have shown that using photometric redshift information and luminosity cuts consistent with the empirical black hole mass – luminosity measurements, one can decrease the number of galaxy counterpart candidates considerably, down to a number $\sim 10^3$–10^4 approximately 10 days before merger, $\sim$ 100–1000 at 1 day, and $\sim$ 1–1000 at ISCO. These galaxies will be typically very faint, with absolute magnitudes between $M_B = (-18,-16,-14)\pm2$ for $M = 10^{5,6,7}\mathrm{M}_\odot$. Moreover, the GW localization volume will enclose $\sim$ 30 quasar counterpart candidates at 10 days before merger, decreasing to $\sim$ 1 quasar close to ISCO. We find that both the orbital inclination and the spins can be measured with GWs to an excellent precision for each counterpart candidate in the field, several months before the merger. Using this information, it may be possible to assess, in advance, which SMBH binaries will receive a recoil with a direction (and known magnitude) that is likely to plunge them into the surrounding gaseous disk, favoring a transient EM signal. If SMBH binary orbits align with the plane of the galactic disk, then measuring the disk orientation to ±20 deg would have a potential for further reducing the number of counterpart candidates by typically more than an order of magnitude.

The best hope to find a merger event EM counterpart may be to look for variable emission produced by gas near the BHs. EM variability can be expected if there is ambient gas surrounding the coalescing binary, on the timescale of the periodic gravitational perturbation, $\sim$ 0.1–10 hr. An electromagnetic transient might take place shortly after the merger due to GW recoil or the sudden central rest-mass loss. The resulting counterpart candidates should be monitored for any type of EM transients or periodic variability whose period and time dependence is correlated with that of the known gravitational perturbation. The basic requirements of a wide field of view, and fast detectors, are similar to those of searches being planned for distant cosmological supernovae. For typical LISA sources, a triggered EM counterpart search campaign will require monitoring a several–square degree area, and could aim for variability at the 24–27 mag level in optical bands, corresponding to 1-10% of the Eddington luminosity for prime *LISA* sources with $\sim(10^6$–$10^7)\,\mathrm{M}_\odot$ BHs at $z = 1-2$, on time–scales of minutes to hours. A cross–correlation of the phase of any variable EM signal with the quasi–periodic gravitational waveform over 10-1000 cycles may aid the detection. The optical emission from near the BHs may be obscured by large columns of gas and dust during the merger, in which case monitoring a similar area, to similar flux levels in X–ray, infrared or radio bands may be required.

The real–time monitoring envisioned here could well make the difference between detecting and missing the prompt EM counterpart. Our results therefore also constitute a strong scientific case for allowing data from LISA to be optionally downloaded on $\sim$ hourly timescales, to permit near–real–time analysis when a particularly interesting event is noticed.

The secure identification of the EM counterpart to a GW event would indeed have far–reaching implications. The identification of a counterpart would provide observational insights into poorly understood processes related to SMBH binary accretion and transients during a general relativistic merger involving the presence of gas. Another tantalizing application of such observations is the possibility to constrain, in new ways, models of gravity on cosmological scales and the geometry of the universe with these events. Comparing arrival times between the EM and GW signals may allow stringent bounds to be placed on the mass of the graviton and could enable empirical tests of Lorentz violations in the gravity sector.

We thank Alessandra Buonanno, Scott Hughes, Frans Pretorius, Abraham Loeb, and András Pál for helpful discussions, and Zsolt Frei, Ryan Lang, Daniel Chung and George Djorgovski for useful comments on the manuscript. BK acknowledges support from the ITC at Harvard University, the Öveges József Fellowship, and OTKA grant no. 68228. KM was supported in part by the National Science Foundation under Grant No. PHY05-51164 (at KITP). ZH acknowledges partial support by NASA through grant NNG04GI88G, by the NSF through grant AST 05-07161, and by the Polányi Program of the Hungarian National Office for Research and Technology (NKTH).

REFERENCES

Armitage, P. J., & Natarajan, P. 2002, ApJ, 567, L9
Armitage, P. J., & Natarajan, P. 2005, ApJ, 634, 921
Artymowicz, P., & Lubow, S. H. 1994, ApJ, 421, 651
Artymowicz, P., & Lubow, S. H. 1996, ApJ, 467, L77
Arun, K. G., Iyer, B. R., Qusailah, M. S. S., & Sathyaprakash 2006a, Class. Quantum Grav., 23, L37
Arun, K. G., Iyer, B. R., Qusailah, M. S. S., & Sathyaprakash 2006a, Phys. Rev. D, 74, 024025
Arun, K. G., Iyer, B. R., Sathyaprakash, B. S., & Sinha, S. 2007, Phys. Rev. D, 75, 124002
Arun, K. G., Iyer, B. R., Sathyaprakash, B. S., Sinha, S., & Van den Broeck, C. 2007, eprint arXiv:0707.3920
Baker, J. G., Centrella, J., Choi, D.-I., Koppitz, M., van Meter, J. R., & Miller, M. C. 2006, ApJ, 653, L93
Baltay et al. 2007, eprint arXiv:astro-ph/0702590
Barack, L.& Cutler, C. 2004, Phys. Rev. D, 69, 082005
Barnes, J. E., & Hernquist, L. 1992, Ann. Rev. Astron. Astrop., 30, 705
Begelman, M. C., Blandford, R. D. & Rees, M. J. 1980, Nature, 287, 307
Bekenstein, J. D. 2004, Phys. Rev. D, 70, 3509
Benson, A. J., Dzanovic, D., Frenk, C. S., & Sharples, R. 2007, MNRAS, 379, 841

Berti, E., Buonanno, A. & Will, C. M. 2005a, Phys. Rev. D71, 084025
Berti, E., Buonanno, A. & Will, C. M. 2005b, Class. Quant. Grav. 22, S943
Berti, E., Cardoso, V., & Will, C. M. 2006, Phys. Rev. D73, 064030
Bode, N. & Phinney, S. 2007, APS April Meeting, http://meetings.aps.org/link/BAPS.2007.APR.S1.10
Bogdanović, T., Reynolds, C. S., & Miller, M. C. 2007, ApJ, 661, L147
Brügmann, B., Gonzalez, J., Hannam, M., Husa, S., & Sperhake, U. 2007, eprint arXiv:0707.0135
Campanelli, M., Lousto, C. O., Zlochower, Y., & Merritt, D. 2007, ApJ, 659, L5
Chung, D. J., Kolb, E. W., & Riotto, A. 2002, Phys. Rev. D, 65, 083516
Csáki, C., Erlich, J. & Grojean, C. 2001, Gen. Rel. Grav. 33, 1921
Coe, D. et al. 2006, AJ, 132, 926
Cornish, N. J., & Porter, E. K. 2006, Class. Quant. Grav., 23, S761
Cornish, N. J. & Rubbo, L. J. 2003, Phys. Rev. D, 67, 022001
Cutler, C. 1998 Phys. Rev. D, 57, 7089
Cutler, C., & Flanagan, È. E. 1994, Phys. Rev. D, 49, 2658
Dalal, N., Holz, D. E., Chen, X., & Frieman, J. A. 2003, ApJ, 585, 11
K. Danzmann, LISA and LISA Pathfinder 2004, (Noordwijk: ESA), www.rssd.esa.int/SP/SP/docs/LISASymposium.../K.Danzmann/KD_LISASymp04.pdf
Deffayet, C. & Menou, K. 2007, ApJ, 668, L143
Dvali, G., Gabadadze, G. & Porrati, M. 2000, Phys. Lett. B, 485, 208.
Dotti, M., Salvaterra, R., Sesana, A., Colpi, M., & Haardt, F. 2006, MNRAS, 372, 869
Dotti, M., Colpi, M., Haardt, F., & Mayer, L. 2007, MNRAS, 379, 956
Dreyer, O., Kelly, B., Krishnan, B., Finn, L. S., Garrison, D. & Lopez-Aleman, R. 2004, Class. Quantum Grav., 21, 787
Dubinski, J., Mihos, J. C., & Hernquist, L. 1996, ApJ, 462, 576
Dubovsky, S. L., Tinyakov, P. G., & Tkachev, I. I. 2005, Phys. Rev. Lett., 94, 181102
Eisenstein, D. J., 1997, eprint arXiv:astro-ph/9709054
Escala, A., Larson, R. B., Coppi, P. S., & Mardones, D. 2004, ApJ, 607, 765
Escala, A., Larson, R. B., Coppi, P. S., & Mardones, D. 2005, ApJ, 630, 152
Ferrarese, L., & Ford, H. 2005, Space Sci. Rev., 116, 523
Ferrarese, L. and Merritt, D., 2000, ApJ, 539, L9
Finn, L. S. 1992, Phys. Rev. D, 46, 5236
Gebhardt, K. et al. 2000, ApJ, 539, L13
González, J. A., Sperhake, U., Brügmann, B., Hannam, M. D., & Husa, S. 2007b, Phys. Rev. Lett., 98, 091101
Graham, A. W., Erwin, P., Caon, N., & Trujillo, I. 2001, ApJ563, L11
Gregory, R., Kaloper, N., Myers, R. C., & Padilla, A. 2007, eprint arXiv:0707.2666
Gualandris, A., & Merritt, D. 2007, in "2007 STScI Spring Symposium: Black Holes", eds. M. Livio and A. M. Koekemoer. (Cambridge University Press) in press, arXiv:0708.3083
Gunnarsson, C., Dahlén, T., Goobar, A., Jönsson, J., & Mörtsell, E. 2006, ApJ, 640, 417
Günther, R., Schäfer, C., & Kley, W. 2004, A&A, 423, 559
Günther, R., & Kley, W. 2002, A&A, 387, 550
Haehnelt, M. G., 1994, MNRAS, 269, 199
Hayasaki, K., Mineshige, S., & Sudou, H. 2007, PASJ, in press, arXiv:astro-ph/0609144
Hellings, R. W. & Moore, T. A. 2003, Class. Quant. Grav. 20, S181
Holder, G., Haiman, Z., & Mohr, J. J. 2001, ApJ, 560, L111
Holz, D. E., & Hughes, S. A. 2005, ApJ, 629, 15
Hughes, S. A., & Menou, K. 2005, ApJ, 623, 689
Hughes, S. A. 2002, MNRAS, 331, 805
Huterer, D., Takada, M., Bernstein, G., Jain, B. 2006, MNRAS, 366, 101
Islam, R. R., Taylor, J. E., & Silk, J. 2004, MNRAS, 354, 629
Jacobson, T., & Mattingly, D. 2004, Phys. Rev. D, 70, 024003
Jensen, E. L. N., et al. 2007, ApJ, in press, arXiv:astro-ph/0704.0307
Kawata, D., & Gibson, B. K. 2003, MNRAS, 346, 135
Keller, S. C., et al. 2007, Publications of the Astronomical Society of Australia, 24, 1, astro-ph/0702511
Kocsis, B., Frei, Z., Haiman, Z. & Menou, K. 2006, ApJ, 637, 27
Kocsis, B., Haiman, Z., Menou, K., & Frei, Z. 2007, Phys. Rev. D, 76, 2003 (Paper I)
Kormendy, J. & Richstone, D. 1995, ARA&A, 33, 581
Lang, R. & Hughes, S. A. 2006, Phys. Rev. D, 74, 122001
Lang, R. & Hughes, S. A. 2007, submitted to ApJ, eprint arXiv:0710.3795
Lin, H., Yee, H. K. C., Carlberg, R. G., Morris, S. L., Sawicki, M., Patton, D. R., Wirth, G., & Shepherd, C. W. 1999, ApJ, 518, 533
MacFadyen, A. I., & Milosavljevic, M. 2006, eprint arXiv:astro-ph/0607467
Madau, P. 1999, eprint arXiv:astro-ph/9907268
Magorrian, J., et al. 1998, AJ 115, 2285
Melia, F. & Falcke, H. 2001, ARA&A, 39, 309
Menou, K., Haiman, Z., & Narayanan, V. K. 2001, ApJ, 558, 535
Micic, M., Holley-Bockelmann, K., Sigurdsson, S., & Abel, T. 2007, MNRAS, 380, 1533
Miller, M. C. 2005, ApJ, 618, 426
Milosavljevic, M., & Merritt, D. 2007, ApJ, 596, 860
Milosavljevic, M., & Phinney, E. S. 2005, ApJ, 622, L93
Misner, C. W., Thorne, K. S., & Wheeler, J. A. 1973, Gravitation (San Francisco: Freeman)
Moore, T. A., & Hellings, R. W. 2002, Phys. Rev. D, 65, 062001
Papaloizou, J. C., Nelson, R. P., & Masset, F. 2001, Astron. & Astrophys. , 366, 263
Pauli, W. & Fierz, M. 1939, Proc. Roy. Soc. (London) A73, 211
Peters, P. C. 1964, Phys. Rev. B 136, 1224
Piro, L., den Herder, J. W., & Ohashi, T. 2007, eprint arXiv:0707.4103
Poisson, E. & Will, C. M., 1995, Phys. Rev. D, 52, 848
Prince, T. A., Tinto, M., Larson, S., L., & Armstrong, J. W., 2002 Phys. Rev. D, 66, 122002
Ryan et al., 2007 ApJ, 668, 839
Sesana, A., Volonteri, M., & Haardt, F. 2007, MNRAS, 377, 1711
Schnittman, J. D., & Buonanno, A. 2007, ApJ, 662, L63
Schutz, B. F. 1986, Nature, 323, 310
Sheth, R. K., et al. 2003, ApJ, 594, 225
Sundelius, B., Wahde, M., Lehto, H. J., & Valtonen, M. J. 1997, ApJ, 484, 180
Trias, M. & Sintes, A. M. 2007, eprint arXiv:0707.4434
Tyson, J. A., & the LSST collaboration 2003, eprint arXiv:astro-ph/0302102
Vasúth, M. & Majár, J. 2007, Int. Jour. of Mod. Phys. A 22, 2405, arXiv:0705.3481
Vecchio, A. 2004, Phys. Rev. D, 70, 042001
Vallisneri, M. 2007, eprint arXiv:gr-qc/0703086
Vallisneri, M., & Cutler, C. 2007, eprint arXiv:0707.2982
Volonteri M., Haardt F., & Madau P., 2003, ApJ, 582, 559
Will, C. M. 2006, Living Rev. Relativity 9, 3. http://www.livingreviews.org/lrr-2006-3